THE LOW-ENERGY CHARGED PARTICLE ENVIRONMENT OF THE EARTH *

by

W. N. Hess, G. D. Mead and M. P. Nakada
Goddard Space Flight Center
Greenbelt, Maryland

* This paper is based in part on a talk given by W. N. Hess at the AIAA Thermophysics Specialist Conference in Monterey, California, September 13-15, 1965, and in part on a paper, "Advances in Particles and Field Research in the Satellite Era", published in Reviews of Geophysics.

I. INTRODUCTION

The object of this paper is to review what we know about the radiation environment of the earth. Emphasis will be placed on the low energy particles that would cause degradation to thermal control surfaces. Protons in the range of 1 Kev to 1 Mev will be discussed and electrons up to 100 Kev or so. These particles form a part of several components of the earth's environment. There are several parts of the radiation environment of the earth, starting from the sun's outer atmosphere, the corona, which blows a particle stream, the solar wind, towards the earth. This solar wind, blowing against the geomagnetic field, distorts it into an elongated cavity called the magnetosphere. Outside this cavity a turbulent regime exists in which energetic particles are born. Inside the cavity are the Van Allen radiation belts.

Let us examine these components of the radiation environment and then decide how much of a problem each of them poses to thermal coatings.

II. THE SOLAR WIND

Before the satellite era, Biermann has conjectured that the explanation of comet tails pointing away from the sun required more than just light pressure and that it was very likely that energetic solar plasma accompanied by magnetic fields was continually present.[1] Parker demonstrated theoretically that the solar corona was unstable and must be expanding continuously.[2,3] He studied the hydrodynamic expansion of the solar corona with a simple spherically symmetric model and was able to deduce plasma velocities and densities from coronal properties. His studies indicated that a continuous wind should exist. He also estimated the strength and direction of the interplanetary field under the assumption that this field was of solar origin and was carried along by the solar wind. Due to the rotation of the sun the solar field lines should have the form of an Archimedes spiral (see Figure 1).

Interplanetary space probes have given striking confirmation to the ideas and calculations of Biermann and Parker.

Gringauz on Lunik II and III measured interplanetary plasma fluxes,[4] but did not measure particle energies and therefore could not differentiate between a light breeze and a solar wind, nor determine the direction of flow. They found fluxes of about 10^8 part/cm^2-sec.

A Faraday cup flown on Explorer X by Bridge and others at MIT confirmed the Lunik fluxes and also indicated a definite wind that came approximately from the sun with a velocity of about 300 km/sec.[5]

More recent measurements by Neugebauer and Snyder[6,7,8] on Mariner II and the MIT[9] and Ames[10] groups on Explorer XVIII (IMP-I) have extended over long enough times to indicate that

1. a definite wind ($\sim$ 300-500 km/sec) blows at all times;

2. the energy spread in the wind is narrow compared to the average directed energy ($\Delta E/E \sim .01$);

3. the wind comes nearly radially from the sun;

4. protons and He nuclei appear to be present (see Figure 2);

5. the wind is very gusty—showing fluctuations in energy, energy spread, and density in times of the order of hours.

Longer term studies with Mariner II results show a striking correlation between geomagnetic activity and daily average solar wind velocity.[8] The correlation between solar wind velocity and the 27-day solar rotation as well as the velocity fluctuations seem to indicate that the wind characteristics depend more on local conditions in the solar corona rather than on over-all solar properties.

III. The Magnetosphere

It has long been realized that plasmas and magnetic fields tend to confine one another. In an experimental machine such as a stellerator, for example, a strong magnetic field can compress and confine a hot dense plasma in a small region of space without walls. In like fashion, if a streaming plasma encounters a magnetic object such as a magnetized sphere, the plasma will confine the magnetic field to a limited region about the object. The object, in turn, will tend to exclude the plasma, creating a hole or cavity. The size of the cavity is determined by the energy density of the streaming plasma and the degree of magnetization of the object.

In addition, if the velocity of the plasma is sufficiently great as to be highly supersonic in the magnetohydrodynamic sense—that is, if the velocity is much higher than the Alfvén velocity in that medium—a detached shock wave may be produced in the region ahead of the cavity boundary. This process is analogous to the formation of the detached shock wave in front of an aerodynamic object traveling at hypersonic speeds (i. e., above Mach 5) through the atmosphere.

In 1931 Chapman and Ferraro first predicted the confinement of the earth's magnetic field inside an elongated cavity during magnetic storms.[17] The continual presence of such a cavity has been experimentally verified by many satellite observations including those of Explorers X, XII, XIV, XVIII (IMP-I) and XXI (IMP-II). Figure 3 shows one radial pass of Explorer XII.

Cahill's magnetometer record[12] shows the expected radial decrease until at 8.2 R_e the field suddenly changes magnitude and starts wandering in direction and strength. At this same radial location the trapped radiation belt flux suddenly fell to essentially zero. The region inside the cavity[13,14] is called the magnetosphere, and the boundary is termed the magnetopause. In addition, Explorer XVIII (IMP-1) has verified the presence of a detached shock wave.[15] The region between the magnetopause and the shock wave is usually referred to as the transition region. Outside this transition region, i.e., beyond the shock wave, conditions are characteristic of the interplanetary medium, and the presence of the magnetized earth has little or no effect.

The dimensions of the cavity depend, of course, on the intensity of the solar wind, although the dependence is rather weak. That is, large changes in the solar wind intensity produce comparatively small changes in the size of the cavity. The distance from the center of the earth to the magnetopause in the solar direction is typically around 10 R_e, although distances less than 8 R_e and more than 13 R_e have occasionally been observed. The shock wave is located several R_e beyond this. At 90° to the solar direction, both the magnetopause and shock wave are observed to flare out todistances about 30-50 percent greater than the subsolar distances. In the anti-solar direction the cavity extends out to very large distances, very likely as far as the moon or further, i.e., 60 R_e. No closure of the magnetosphere tail has yet been observed by satellites.

Mead[16] has calculated the shape of the field lines in the noon-midnight meridian shown in Figure 4 by assuming specular reflection of the solar wind, no external field, and pressure balance at each point on the surface. However, these calculations are based on assumptions which are not entirely met. First of all, the solar wind is not field-free, but contains an imbedded field averaging about 5γ. Since the solar wind is therefore supersonic in the magnetohydrodynamic sense, a shock wave is formed ahead of the boundary. In the transition region, the solar wind flow is no longer directional, but becomes disordered and randomized.

In addition, Dungey has suggested that if the interplanetary field has a southward component, some of the earth's field lines would interconnect with the interplanetary field, thus modifying the field topology.[17] Axford and Petschek have suggested that dissipative forces near the boundary would cause the polar field lines to be drawn back into a very long magnetosphere tail, with the outward-directed field lines being separated from the inward-directed ones by a neutral sheet[18] (Figure 5). Ness has found evidence from IMP-1 data for the existence of such a sheet.[19] Dessler,[20,21] Beard,[22] Axford and Hines,[23] Spreiter and Jones,[24] and others have discussed various modifications to the simple Chapman-Ferraro model. Most of the discussion, however, has been qualitative, rather than quantitative in nature, because of the great difficulty in incorporating the newer ideas into a complete mathematical magnetosphere theory.

The first definite observation of the magnetospheric boundary was made with Explorer X, launched on March 25, 1961, into a highly elliptical orbit with an apogee of 47 earth radii, approximately in the anti-solar direction. Between distances of 22 R_e and apogee, the satellite apparently crossed the boundary (or vice versa) on six principal occasions. This conclusion was reached after comparing the results of the rubidium vapor magnetometer experiment of Heppner et al. at Goddard[25] with the plasma probe experiment of Bridge et al.[5] at MIT. While inside the magnetosphere, the magnitude of the field was comparatively strong (20-30 gammas), and there was usually no detectable plasma. Outside the boundary the field changed directions and became weaker (10-15γ), and plasma was always observed. The position of the satellite at the times during which the boundary crossings were observed indicated that if the magnetosphere tail was symmetric about the sun-earth line, the dimensions of the cavity would be somewhat broader than the current theories had indicated; i.e., about 50 R_e in diameter, as opposed to the predicted 35-40 R_e.

Since Explorer X was battery-operated, it only transmitted during its first outbound pass, and no further data was received. Explorer XII was launched August 16, 1961, in a generally solar direction with an apogee of 13.1 R_e. A three-element flux gate magnetometer provided by Cahill at the University of New Hampshire[12] was one of the various experiments on board. This instrument was capable of detecting the

magnitude and direction of fields between 10 and 1,000 gammas. The satellite had a period of 26-1/2 hours and, while apogee remained within about 60° of the solar direction, crossings of the magnetosphere boundary were observed twice during each orbit, once on the outbound and once on the inbound pass. The most obvious characteristic of the boundary was a sudden change in direction of the magnetic field, with the direction and magnitude of the field much more variable outside the boundary. Usually, but not always, this was accompanied by a decrease in the magnitude of the field outside the boundary. An example of a typical pass is shown in Figure 3. The outer shock wave boundary was not observed, since it was usually beyond apogee.

IV. THE TRANSITION ZONE AND SHOCK WAVE

The IMP-I (Exp. 18) satellite was launched in November 1963 into a highly eccentric orbit going out to 30 R_e with instruments on board designed to explore the outer magnetosphere and interplanetary region. This satellite discovered a new and interesting feature of the terrestrial environment. Two instruments on IMP I showed the existence of a detached bow shock wave towards the sun from the magnetopause. The magnetometer flown by Ness[15] (capable of measuring fields with a sensitivity of 1/4) showed two transitions as it moved radially away from the earth. As an example on orbit 11 (see Figure 6) at about 13.6 R_e the satellite

passed out through the magnetopause into a region of disordered field of from 0-15γ, with variable direction. Then at 20 R_e a second transition occurred, and outside this the field became quite steady at about 4γ. This second transition indicates a shock wave. The magnetic field in the solar wind outside the shock is rather steady and then suddenly, in a few thousand kilometers, the field changes character significantly and becomes turbulent and disordered. The variance of the field (the RMS deviation of a 5 minute set of data) is very small outside the transition and is relatively large inside the shock.

Even before the IMP-I results were obtained, the suggestion had been made in analogy to supersonic aerodynamics, that there might be such a detached shock wave upstream of the earth. Figure 7 shows the detached shock wave ahead of a sphere immersed in a supersonic flow of gas. The analogy with the magnetosphere however is quite imperfect. In aerodynamics the shock wave results from collisions of particles and is about one mean free path thick. In the solar wind a coulomb-collision mean free path ($\gamma = 1/n\sigma \sim 10^{+14}$ cm) is so large that collisions play no part in the observed shock wave. This collisionless shock wave is produced by the action of the magnetic field, and the characteristic dimension is the cyclotron radius, not the mean free path. A 1 kev proton in a field of 10γ has a cyclotron radius of 450 km. Inside a detached supersonic aerodynamic shock, ahead of the obstacle the regime is turbulent. This appears to be the case for the magnetospheric detached collisionless shock wave also.

The MIT plasma detector on IMP-I also observed the shock wave.[9] Outside the shock near apogee the detector, a multi-grid faraday cup, showed a narrow well-collimated beam of solar wind moving radially away from the sun. A typical measured proton flux was 10^8 p/cm^2-sec. The wind usually appeared all in one energy window, e.g., from 220 to 640 ev. At the same place that the magnetometer showed the change in character of the magnetic field the solar wind also changed. Outside the shock the plasma is unidirectional flowing from the sun (see Figure 8). Inside the shock near the subsolar point the plasma is more nearly isotropic. On the sides of the magnetosphere the flow becomes more directed, flowing backwards along the sides. Besides this change in directionality the protons change in energy too. In the transition zone between the shock and the magnetopause are protons of both considerably higher and lower energy and also of lower energy than in the solar wind. All channels of the MIT detector show significant proton fluxes in the transition zone. The Ames plasma detector,[10] a multichannel electrostatic analyzer, showed the change in proton energy too (see Figure 9). This detector indicates the flow in the transition region is somewhat anisotropic even near the subsolar point. These two experiments show that in the transition zone the proton energy spectrum extends from $0.1 < E < 5$ kev. Apparently the plasma has been thermalized in this region. It is nearly monoenergetic outside the shock and roughly Maxwellian in the transition zone. Shock waves normally produce an increase in entropy. The change in both the proton energies and angular distribution indicates an increase in disorder, and therefore an increase in entropy inside the bow shock.

Electrons have not yet been observed in the solar wind, although they must be there for the plasma to be electrically neutral. If they have the same velocity as the protons in the wind they would have an energy of about 1 ev, and no instruments so far flown would have detected them. The MIT plasma probe[9] had a channel to count electrons of $65 < E_e < 210$ ev. It detected no electrons outside the shock, but inside the shock a flux of $\sim 10^8$ electrons/cm^2-sec in this energy range was usually found. These are apparently solar wind electrons accelerated in the transition zone. Freeman earlier had detected a flux of $\sim 10^{10}$ electrons/cm^2-sec of 200 ev $< E_e <$ 500 kev outside the magnetosphere with a CdS detector on Explorer XII.[26] This energetic electron flux extended out about 20,000 km beyond the magnetopause on to just about the shock position. It seems quite apparent that these electrons are the same population observed by the MIT plasma probe on IMP. The Goddard retarding potential analyzer on IMP-I also detected a substantial electron flux in the transition zone.[27] The flux measured by this instrument was isotropic and consisted of $\sim 10^8$ electrons/cm^2-sec of $E > 100$ ev.

The magnetopause may not really exclude all the plasma striking it from outside. Measurements by Serbu on IMP I show that the electron flux in the energy range $5 < E < 100$ ev does not show a discontinuity at the magnetopause, while the solar wind proton flux of Bridge does fall off sharply inside this boundary. The boundary seems to be semi-permeable, allowing electrons to flow inwards, but not protons. This would suggest certain instabilities at the boundary which are mass-sensitive.

Higher energy electrons were observed on IMP-I. A solid state detector of Simpson's group[28] and a Geiger counter of Anderson[29] showed that fluxes of E > 40 Kev electrons were present intermittently. Anderson found peaks of $\varphi \sim 10^6$ electrons/cm^2-sec lasting the order of minutes (see Figure 10). These usually occurred in the transition zone close to the magnetopause. None were observed near apogee on early orbits. Anderson has suggested that these particles are sloughed off from the magnetosphere and had previously been trapped particles. Simpson suggested they were at the shock location and might be locally accelerated in the shock. Jokipii and Davis[30] have showed that it is unlikely that the particles would be observed at the shock location. Acceleration by a factor of 2 or 3 is possible at the shock, but this is clearly not enough to produce 40 kev electrons. The particles should be carried along with the bulk velocity of the solar wind and should be observed at all places downstream of the source location, not just at the shock. Jokipii suggests the particles may be Fermi-accelerated in the transition zone, and also that the magnetic field geometry may be such that local trapping occurs to produce large local fluxes resembling the observed spikes. There is no quantitative theory of the origin of these energetic electrons.

The electron measurements described here all were made at small SEP (sun-earth-probe) angles. Data taken at larger SEP angles show other features of the shock and transition zone. Figure 11 shows the location

of the magnetopause and shock as measured by the magnetometer for the first 48 orbits of IMP-1. The curve through the magnetopause points is the theoretical shape of the boundary as calculated by the single-particle reflection model. The agreement is quite good at least to 90° SEP. At larger angles, the magnetopause is observed to flare out more than the single-particle theory predicts. The curve through the shock wave points is the theoretical curve for an aerodynamic shock wave of mach number 8 for a gas of $\gamma = 5/3$. In this plasma situation the Mach number is replaced by the Alfvén number = V_w/V_A. For the interplanetary medium the Alfvén velocity is roughly $V_A = 50$ km/sec, so the Alfvén number of the solar wind is about 8.

A summary of the large scale magnetic and particle environment of the earth is shown in Figure 12. The solar wind blowing on the geomagnetic field creates the magnetosphere cavity and the bow shock wave upstream of the cavity. Inside this is the terrestrial environment including the radiation belt. Outside this is the solar environment.

V. RADIATION BELTS

In 1958, when Explorer I was launched with a geiger counter on board, it discovered a region of high count rate starting at about 1000 km altitude. This was unexpected. In fact, it was suggested that the

counter might have malfunctioned. But when Explorer III showed the same results a little later, it was demonstrated that the effect was real. Van Allen, who had conducted the experiments on Explorer I and Explorer III, realized very soon that the measured high count rates were due to charged particles trapped in the earth's magnetic field.(31) Störmer had worked extensively on this general subject(32) and even calculated orbits of trapped particles years earlier, but the actual existence of a terrestrial ring current had also essentially included the idea of trapped particles.(33)

At the same time that these experiments in space were going on, experiments with trapped particles were being conducted in various laboratories. Project Sherwood is an attempt by the AEC to make a controlled thermonuclear reaction on a small scale by confining charged particles in a magnetic field. Christofilos, who was working on Sherwood, extrapolated the laboratory idea to earth scale and suggested the possibility of trapping a large number of charged particles in the magnetic field of the earth by using a nuclear explosion to inject the particles.(34) This idea was carried out in the Argus experiment and demonstrated experimentally that charged particles could really be trapped in the earth's field.

From a study of the Explorer I data, Van Allen showed that the particles counted were geomagnetically trapped. Data taken at different longitudes looked quite different when plotted in terms of geographic coordinates, but when replotted in terms of geomagnetic coordinates the

different sets of data agreed. Later McIlwain developed an especially useful set of magnetic coordinates, the B-L system, which is now normally used in plotting radiation belt data.[35] This system takes data collected in geographic coordinates and combined data at different longitudes to make a two dimensional presentation of the data. In a dipole field L is the geocentric distance to the equatorial crossing of a field line in units of earth radii and B is the value of the magnetic field strength. For the earth's field the definition of L is more complicated but fundamentally similar.

The data from Explorer IV and Pioneer III allowed Van Allen[36] to show the existence of two radiation belts (see Figure 13). This is really only the case for particles that can penetrate 1 gm/cm^2, and we know now that the two zones are made up of different kinds of particles--protons in the inner zone and electrons in the outer zone. A comparison of Pioneer III and IV data showed the time variability of the outer zone.

The data obtained by these various satellites before 1960 enabled one to give general spatial limitations and time variability of the radiation belt and say something about the penetrability of the radiation, but one did not know what kind of particles were being counted.

Later experiments using detectors that identified particles and measured their energies have enabled us to get fairly good spatial

maps of several different components of the radiation belt. Figures 14 to 17 show four typical populations. In Figures 14 and 15 are shown maps of the high energy inner zone protons and high energy outer zone electrons that together make up the particles counted by Van Allen's detectors on Explorer 4 and Pioneer 3 that are shown in Figure 13. Figure 16 shows the electron population for E > 40 Kev. This electron flux (and the higher energy Figure 15 electrons also) vary considerably with time. Magnetic storms can produce changes of a factor of 10 or more in both of these. In Figure 17 is shown a map of low energy protons, which are mostly in the outer zone.

In the inner zone, there are protons with energies up to hundreds of Mev. In the outer zone, proton energies are much lower, fluxes are much higher, and albedo neutrons are inadequate by many orders of magnitude for a satisfactory accounting of the observed fluxes.

These outer zone protons were discovered in 1962 by Davis and Williamson[37] with equipment on Explorer XII. Observations of these protons have also been made on Explorers XIV and XV. A rather surprising result of measurements over a few years has been the stability of a major fraction of these protons, although fluxes are large and proton lifetimes relatively short.

Because of this stability, it has been possible to obtain relatively detailed information on the energy spectra and directional fluxes. The detectors measured protons with energies between 100 kev and 5 Mev.

Most of the protons were near the lower energy limit. The data was adequately ordered through the use of L and equatorial pitch angle (EPA), as calculated with the Jenson and Cain earth's magnetic field,[38] for $L < 5$. For EPA = 90°, a peak intensity of 3.7×10^{7} protons/cm^2-sec-ster has been found, with a gradual falloff in intensity at both larger and smaller L. At any L, the peak intensity was found for EPA = 90°, with a smooth fall off to zero at small EPA.

The energy spectra were found to have large but smooth variations with both L and EPA (see Figure 18). More energetic protons were found near the earth and at large EPA. The spectral data was well represented by e^{-E/E_0} where E_0 varied as L^{-3} for EPA = 90° and varied less rapidly with L for smaller EPA.

Theoretical studies[39] indicate that these spectral variations can be explained through a simple model that assumes that the source of these protons is at or near the magnetopause. The protons are assumed to migrate rapidly in L space through the violation of the third adiabatic invariant for trapped particles, but with the preservation of the magnetic moment μ and line integral I invariants. As the protons drift inwards they are accelerated, the exponential spectrum gets harder, and the value of E_0 increases. For EPA = 90° the field $B \propto L^{-3}$, and $E_0 \propto B \propto L^{-3}$, in agreement with the experimental data (see Figure 19).

Other studies indicate that L-space motion through geomagnetic field changes such as sudden commencements and sudden impulses may be adequate to explain the variations in fluxes with L when loss processes are also included.[40]

Observations at L values between 5 and 8 indicate that large time variations do occur for protons with energies greater than 1 Mev, but that protons near 100 kev are relatively more stable. As expected, the data at these larger values of L are not well ordered by magnetic field models that do not take into account perturbing fields such as those produced by the solar wind at the magnetopause.

Because of the large energy density of these outer belt protons, the hope arose that these protons might be the cause of the ring current. However, calculations with measured fluxes indicate that these protons make only about a 10γ disturbance field at the earth's surface.[41]

In 1959 a rocket carrying an electron spectrometer showed that the penetrating particles in the outer belt were electrons.[40] An outstanding difference between electrons and protons in the outer zone is the large (factors of 100) variability in the electron fluxes in times of the order of hours.[43] Detectors on Explorer VI showed that electron flux changes were large, especially at the times of magnetic storms. The $E > 1.5$ electrons at about $L = 3$ frequently decrease, sometimes nearly disappearing, during a large storm, while the low energy $E > 40$ kev flux may increase. McIlwain[44] showed how the $E > .5$ Mev electrons

injected into the field by a nuclear explosion behaved during storms (see Figure 20). Several storms decreased the flux at $L \sim 4$, but then in December 1962 the flux increased by a factor of about 100.

O'Brien showed on Injun I and III that there were frequently large fluxes of precipitated electrons striking the upper atmosphere in the region of the outer belt.[45,46] At the auroral zone there is always precipitation. He showed that outer belt trapped fluxes increased when precipitation increased, leading to the splash-catcher model of the outer belt. It would seem that there might be a common source for the aurora, precipitated electrons, and outer belt trapped particles.

We know something about radiation belts on some other planets. Decimeter radio radiation from Jupiter[47] has been identified as being synchrotron radiation from trapped electrons.[48] It shows linear polarization and the radio source is more than three times the width of the planet;[47] both facts are in keeping with a radiation belt source. If the surface magnetic field is about 10 gauss, as is suggested from other Jupiter radio waves, then the belt should consist of about 10^8 electrons/cm^2-sec of $E > 10$ Mev at about 2 $R_{J\mu}$ to give the observed synchrotron radiation.[50] This is a very intense electron belt compared to the earth's. The synchrotron radiation from the terrestrial natural Van Allen belt is too low to be measured. Synchrotron radiation, however, was measured from the artificial belt formed by the Starfish event.

The Mariner II probe passed about 40,000 km away from Venus on the sunward side. At this distance there was no evidence for a planetary magnetic field[12] or any evidence of trapped particles.[51,52] This does not eliminate the possibility of a radiation belt, but only means that Mariner stayed outside the Venusian magnetosphere and that therefore, the Venus surface field can be no greater than about 10% of the earth's. The Mariner IV flyby of Mars in July, 1965, showed that it too had no discernible magnetic field, and therefore no radiation belts.

There is no evidence of the existence of any other radiation belts. Lunik II showed that the moon's field is less than 100γ, so that it can hardly have a radiation belt.[53] No other planets show significant synchrotron radiation.

VI. THE AURORA

The particles which contribute most to auroral emission have been found to be electrons with energies below 25 kev. However, electrons with energies above 25 kev and with energies as high as 100 kev are also associated with aurorae. Most of the auroral light seems to be produced by electrons near 10 kev. Certain auroras are excited by both electrons and protons, and others appear to be excited predominantly by either electrons or protons.

McIlwain,[54] Davis,[55] and McDiarmid[56] have flown rockets into active auroral displays, and have found that electrons of a few kev are the commonly-found particles. The narrowness of some auroral arcs agrees with electrons being the active particles--the proton cyclotron radius would be larger. The common altitude of visual aurorae of 100 km is what is expected for electrons of about 5 kev. A spectrometer flown by Bloom on a Discoverer satellite showed that electrons up to 150 kev are frequently found in the auroral zone.[57] Brown[58] and Anderson[59] have observed x-rays from detectors on balloons from such electrons.

Recent experiments by Evans' group[60] on Air Force satellites have measured the electron energies down to 80 ev. They show that there are usually fewer electrons at these energies than at 1 kev.

Both magnetic field and trapped particle measurements have made it possible to follow field lines from where auroras occur. These studies show that many auroras occur on field lines that contain trapped particles and that connect directly to the opposite hemisphere. However, many auroras appear to occur near the outer limit of trapping field lines.

Early low-altitude satellites detected large fluxes of electrons with sufficient particle energies to contribute to the production of auroras. The hope arose that fluxes large enough to explain aurorae might exist at higher altitudes; then, some mechanism for the dumping of the trapped electrons from the Van Allen belts was all that would be required for the explanation of aurorae. However, measurements both by Russian[61] and U. S. scientists[62] indicated that although the

higher altitude fluxes were larger, they were insufficient to account for aurorae. A flux tube of the Van Allen belt would be drained in a matter of seconds by a strong aurora; but such an aurora can last hours. A most significant finding by O'Brien[63] was the discovery on Injun of the increase in the trapped particle population when large fluxes of electrons entered the atmosphere (See Figure 21). Thus the elimination of the auroral theory of the dumping of trapped particles has given rise to the view that whatever causes aurorae is also a major contributor to radiation belt population.

Satellites have been equipped with sensitive optical sensors to observe auroras from above.[63] Although these satellites do not stay in the auroral regions very long, they have the advantage of no cloud interference and the ability to scan large areas. These sensors have shown that over some 5° of latitude over the auroral zones, auroras were detected at all times; in the 5° latitude strips bordering the main auroral zone, auroral emissions were detected a large fraction of the time.

VII. LOW ENERGY PARTICLES

Besides the particles we have considered so far in the radiation belt there are large numbers of lower energy particles that we should consider because they can still be damaging to thermal coatings.

Freeman[64] has measured a large flux of protons of 1/2 Kev < E < 1 Mev in the inner belt, using a cadmium sulfide detector on Injun 1. He found fluxes up to 10^{10} protons/cm^2-sec. Hilton et al.,[65] using a faraday cup on a low altitude polar-orbiting satellite, reported similar fluxes to Freeman's in the energy region 1 to 10 Kev. However, both of these results must be considered tentative. If these large fluxes of trapped protons existed there should be large geophysical effects produced by them. Among other effects, there should be a considerable decrease in the surface geomagnetic field due to the diamagnetic effect of the particles. During the main phase of a magnetic storm the surface field is decreased. This is generally attributed to a "ring current" around the earth. The current is thought to be due to the drift in longitude of trapped particles. Storms sometimes produce changes in the earth's field of as much as one-half percent. To do this requires fluxes of particles just about as detected by Freeman and Hilton. So in fact we do expect these particles to be around part of the time. But big magnetic storms are not very frequent, so we should not have these large proton fluxes very often. This subject must be considered incomplete. We really don't know very much about the proton flux of E < 100 Kev in the radiation belt yet. We can expect some surprises here.

Frank[66] has made a summary of what is known about low energy particle fluxes in Figure 23. He has not shown the inner belt proton fluxes--probably because they are controversial--but they should not

be forgotten. He has shown the thermalized solar wind in the transition zone and the proton fluxes observed on the back side of the magnetosphere by Gringauz[61] and Freeman.[26]

VIII. SUMMARY

Let us now assess the potential damage to thermal coatings that may be caused by these various low energy particle fluxes. To do this we will use a very loosely defined "flux to damage". We will say that the following integrated particle fluxes, φ, will cause significant surface damage (without getting involved in a discussion of the damage mechanisms).

Integrated Fluxes to Damage

$\varphi_p = J_p t = 10^{16}$ protons/cm^2 of 1 kev $< E_p <$ 10 kev

$\varphi_p = J_p t = 10^{14}$ protons/cm^2 of 1 kev $< E_p \sim$ 1 Mev

$\varphi_e = J_e t = 10^{15}$ electrons/cm^2 of 1 kev $< E_e \sim .1$ Mev

These fluxes may not be very good and should be taken with a grain of salt. Using these values of φ and the values of particle fluxes J that we have discussed in earlier sections we can calculate a "time to damage" for several components of the radiation environment. These times are shown in Table 1. It should be understood that these times are by no means exact. They are only meant as order of magnitude indications of the kinds of problems involved. To find a quantitative change in surface absorbence or reflectance the particle flux should be integrated over the satellite orbit and the energy spectrum

obtained, then multiplied by a quantitatively determined degradation factor to find out what surface changes will occur. The fact of interest shown in Table 1 is that some of the times to damage are measured in years and some in days. This sorts out those components of the radiation environment that will produce a significant effect on surfaces in times of interest and are therefore deserving of further study.

LIST OF ILLUSTRATIONS

Figure

1 The spiral form of the interplanetary magnetic field lines caused by the radial outflow of solar wind and rotation of the sun.

2 Typical energy spectra of the solar wind as measured on Mariner II in 1962. The second peak sometimes present is very likely due to the presence of the He nuclei along with the protons.

3 Magnetic field data from Explorer XII showing an abrupt change in the field at 8.2 R_e. This change, the magnetopause, is the outer limit of the geomagnetic field.

4 Theoretical shapes of distorted geomagnetic field lines in the magnetosphere noon-midnight meridian plane. The dotted lines are dipole field lines shown for comparison.

5 A theoretical model of the tail of the magnetosphere. Friction at the magnetopause pulls the field lines back and produces a neutral sheet.

6 Magnetic field data from orbit 11 of Explorer XVIII (IMP-I). The magnetopause is at 13.6 R_e. The second transition at

20 R_e to an ordered field outside is the location of the bow shock wave.

7 A sphere in a supersonic wind tunnel showing a detached shock wave upstream from the object.

8 Solar wind data from the MIT plasma probe on IMP-I. In the interplanetary medium the detector shows large fluxes in only one energy channel. In the transition zone there are significant fluxes in all channels (including the electron one).

9 Solar wind data from the Ames plasma detector on IMP-I. The inner boundary of the wind at 11 R_e is approximately at the magnetopause. The sharp transition at 16 R_e is the bow shock wave location. In the transition region protons of all energies are present. In the interplanetary medium protons are only present in one channel.

10 Flux of E > 40 Kev electrons detected on IMP-I. The radiation belt is present inside the magnetopause at 10 R_e, and outside this occasional "islands" of particles are observed.

11 The location of the magnetopause and bow shock as determined by the magnetometer on IMP-I. Shown for comparison are the theoretically expected locations.

12 A summary of the magnetic and particle environment of the earth.

13 Van Allen's picture of the inner and outer zone of the radiation belt made after Pioneer III.

14 The spatial distribution of protons of E 30 Mev. This population is quite stable in time.

15 The spatial distribution of electrons of E 1.6 Mev. This population frequently varies by more than one order of magnitude, up or down.

16 The spatial distribution of electrons of E > 40 Kev. This population often varies by one order of magnitude.

17 The spatial distribution of protons of .1 E 5 Mev. This population is quite stable in time.

18 Energy spectra of low-energy protons measured by Explorer XII at several locations in the outer zone of the radiation belt.

19 The dotted lines are theoretical curves showing how the e-folding energy E_o should vary assuming the outer zone protons move radially, conserving μ and I. The solid lines are the experimental values of E_o from Explorer XII data.

20 Time variations of $E > .5$ Mev electrons in the outer zone measured on Explorer XV.

21 Simultaneous observation of trapped electrons, dumped electrons, and auroral light emission. These and other studies indicate an increasein trapped radiation when aurorae occur.

22 Sample of precipitated flux. Note that near $L = 6$ some precipitated flux is observed at all times since all observations show more than background fluxes.

BIBLIOGRAPHY

1. Biermann, L., Kometenschweife und solare korpuskularstrahlung, Z. Astrophys. 29, 274-286, 1951.
2. Parker, E. N., Dynamics of the interplanetary gas and magnetic fields, Astrophys. J. 128, 664-676, 1958.
3. Parker, E. N., The hydrodynamic theory of solar corpuscular radiation and stellar winds, Astrophys. J. 132, 821-866, 1960.
4. Gringauz, K. I., V. V. Bezrukikh, V. D. Ozerov, and R. E. Rybchinskii, A study of the interplanetary ionized gas, high-energy electrons, and corpuscular radiation from the sun by means of the three electrode trap for charged particles on the second Soviet cosmic rocket, Dokl. Akad. Nauk. SSSR 131, 1301; Soviet Physics Dokl. 5, 361-364, 1960.
5. Bonetti, A., H. S. Bridge, A. J. Lazarus, B. Rossi, and F. Scherb, Explorer 10 plasma measurements, J. Geophys. Res. 68, 4017-4063,
6. Neugebauer, M. and C. W. Snyder, Solar plasma experiment: preliminary Mariner II observations, Science 138, 1095-1097, 1962.
7. Snyder, C. W. and M. Neugebauer, Interplanetary solar wind measurements by Mariner II, Space Research IV, ed. by P. Muller, 89-113, 1964.
8. Snyder, C. W., M. Neugebauer and U. R. Rao, The solar wind velocity and its correlation with cosmic ray variations and with solar and geomagnetic activity, J. Geophys. Res. 68, 6361-6370, 1963.
9. Bridge, H., A. Egidi, A. Lazarus, E. Lyon and L. Jacobson, Preliminary results of plasma measurements on IMP-A, Space Research V, 969-978, 1965.

10. Wolfe, J. H., R. W. Silva, and M. A. Myers, Observations of the solar wind during the flight of IMP-I, J. Geophys. Res., 71, 1319-1340, 1966.

11. Chapman, S., and V. C. A. Ferraro, A new theory of magnetic storms, Terrestrial Magnetism and Atmospheric Elec. 36, 77-97, 171-186, 1931; 37, 147-156, 421-429, 1932; 38, 79-96, 1933.

12. Cahill, L. J., and P. J. Amazeen, The boundary of the geomagnetic field, J. Geophys. Res. 68, 1835-43, 1963.

13. Johnson, F. S., The gross character of the geomagnetic field in the solar wind, J. Geophys. Res. 65, 3049, 1960.

14. Beard, D. B., The interaction of the terrestrial magnetic field with the solar corpuscular radiation, J. Geophys. Res. 65, 3559-3569, 1960.

15. Ness, N. F., C. S. Scearce, and J. B. Seek, Initial results of the IMP-I magnetic field experiment, J. Geophys. Res. 69, 3531-3569, 1964.

16. Mead, G. D., Deformation of the geomagnetic field by the solar wind, J. Geophys. Res. 69, 1181-1195, 1964.

17. Dungey, J. W., Interplanetary magnetic field and the auroral zones, Phys. Rev. Letters 6, 47, 1961.

18. Axford, W. I., H. E. Petschek, and G. L. Siscoe, Tail of the magnetosphere, J. Geophys. Res. 65, 3559-3568, 1960.

19. Ness, N. F., The earth's magnetic tail, J. Geophys. Res. 70, 2989-3005, 1965.

20. Dessler, A. J. and R. D. Juday, Configuration of auroral radiation in space, Planetary and Space Science 13, 63-72, 1965.

21. Dessler, A. J., Length of magnetospheric tail, J. Geophys. Res. 69, 3913-3918, 1964.

22. Beard, D. B., The effect of an interplanetary magnetic field on the solar wind, J. Geophys. Res. 69, 1159-1168, 1964.

23. Axford, W. I., and C. O. Hines, Unifying theory of high latitude geophysical phenomena and geomagnetic storms, Can J. Phys. 39, 1433-1464, 1961.

24. Spreiter, J. R., and W. P. Jones, On the effect of a weak interplanetary magnetic field on the interaction between the solar wind and the geomagnetic field, J. Geophys. Res. 68, 3555-3565, 1963.

25. Heppner, J. P., N. F. Ness, T. L. Skillman, and C. S. Scearce, Explorer 10 magnetic field measurements, J. Geophys. Res. 68, 1-46, 1963.

26. Freeman, J. W., Jr., The morphology of the electron distribution in the outer radiation zone and near the magnetospheric boundary as observed by Explorer 12, J. Geophys. Res. 69, 1691-1724, 1964.

27. Serbu, G. P., Results from the IMP-I retarding potential analyzer, Space Research V, 564-574, 1965.

28. Fan, C. Y., G. Gloeckler, and J. A. Simpson, Evidence for > 30 Kev electrons accelerated in the shock transition region beyond the earth's magnetospheric boundary, Phys. Rev. Letters 13, 149-153, 1964.

29. Anderson, K. A., H. K. Harris, and R. J. Paoli, Energetic electron fluxes in and beyond the earth's outer magnetosphere, J. Geophys. Res., 70, 1039-1050, 1965.

30. Jokipii, J. R., and L. Davis, Jr., Acceleration of electrons near the earth's bow shock, Phys. Rev. Letters, 13, 739-741, 1964.

31. Van Allen, J. A., First public lecture on the discovery of the geomagnetically trapped radiation, State Univ. of Iowa Report SUI 60-13, 1960.

32. Störmer, C., The Polar Aurora, Clarendon Press, Oxford, 1955.

33. Singer, S. F., A new model of magnetic storms, Trans. Am. Geophys. Union 38, 175, 1957.

34. Christofilos, N. C., The Argus experiment, J. Geophys. Res. 64, 869, 1959.

35. McIlwain, C. E., Coordinates for mapping the distribution of magnetically trapped particles, J. Geophys. Res. 66, 3681, 1961.

36. Van Allen, J. A. and L. A. Frank, Radiation around the earth to a radial distance of 107,400 km, Nature 183, 430, 1959.

37. Davis, L. R., and J. M. Williamson, Low energy trapped protons, in Space Research III, 365, 1963.

38. Jensen, D. C. and J. C. Cain, An interim geomagnetic field, abstract, J. Geophys. Res. 67, 3568, 1962.

39. Dungey, J. W., W. N. Hess and M. P. Nakada, Theoretical studies of protons in the outer radiation belts, in Space Research V, 399-403, 1965.

40. Nakada, M. P., and G. D. Mead, Diffusion of protons in the outer radiation belt, J. Geophys. Res. 70, 4777-4791, 1965.

41. Hoffman, R. A., and P. A. Bracken, Magnetic effects of the quiet time proton belt, J. Geophys. Res. 70, 3541-3556, 1965.

42. Cladis, J. B., L. F. Chase, W. L. Imhof and D. J. Knecht, Energy spectrum and angular distributions of electrons trapped in the geomagnetic field, J. Geophys. Res. 66, 2297, 1961.

43. Forbush, S. E., G. Pizzella and D. Venkateson, The morphology and temporal variations of the Van Allen radiation belt October, 1959 to December, 1960, J. Geophys. Res. 67, 3651, 1962.

44. McIlwain, C. E., The radiation belts, natural and artificial, Science 142, 355-361, 1963.

45. O'Brien, B. J., Lifetimes of outer zone electrons and their precipitation into the atmosphere, J. Geophys. Res. 67, 3687, 1962.

46. O'Brien, B. J., High latitude geophysical studies with Injun 3 (3) precipitation of electrons into the atmosphere, J. Geophys. Res. 69, 13, 1964.

47. Sloanaker, R. M., Apparent temperature of Jupiter at a wave length of 10 cm, Astronomical J. 64, 346, 1959.

48. Drake, F. D. and H. Hvatum, Non-thermal microwave radiation from Jupiter, Astronom. J. 64, 329, 1959.

49. Radhakrishman, V., and J. A. Roberts, Polarization and angular extent of the 960 Mc/s radiation from Jupiter, Phys. Rev. Let. 4, 493, 1960.

50. Chang, D. B. and L. Davis, Synchrotron radiation as the source of Jupiter's polarized decimeter radiation, Astrophys. J. 136, 657, 1962.

51. Anderson, H. R., Energetic particles measured near Venus by Mariner 2, J. Geophys. Res. 69, 2651, 1964.

52. Van Allen, J. A. and L. A. Frank, The mission of Mariner 2 preliminary observations: the Iowa radiation experiment, Science 138, 1097, 1962.

53. Dolginov, S. Sh., E. G. Evoshenko, L. N. Zhuzgov, N. V. Pushkov and L. O. Tyurmina, Measuring the magnetic fields of the earth and moon by means of Sputnik III and Space Rockets I and II, Space Research I, 863, 1960.

54. McIlwain, C. E., Direct measurements of particles producing visible auroras, J. Geophys. Res. 65, 2727-2747, 1960.

55. Davis, L. R., O. E. Berg, and L. H. Meredith, Direct measurements of particle fluxes in and near auroras, Space Research, edited by H. K. Kalmen-Bijl, North-Holland Publishing Co., Amsterdam, 721-735, 1960.

56. McDiarmid, I. B., D. C. Rose, and E. Budzinski, Direct measurements of charged particles associated with auroral zone radio absorption, Can. J. Phys. 39, 1888-1900, 1961.

57. Mann, L. G., S. D. Bloom, and H. I. West, Jr., The electron spectrum from 90 to 1200 kev as observed on Discoverer satellites 29 and 31, Space Research III, edited by W. Priester, North-Holland Publishing Co., Amsterdam, 447-462, 1963.

58. Brown, R. R., Balloon observations of auroral zone x-rays, Proc. of the International Conference on Cosmic Rays and the Earth Storm, Kyoto, Sept. 4-15, 1961, I. Earth Storm, 236, 1962.

59. Anderson, K. A., Balloon observations of x-rays in the auroral zone I and II, J. Geophys. Res. 65, 551 and 65, 3521, 1960.

60. Sharp, R. D., J. E. Evans, W. L. Imhof, R. G. Johnson, J. B. Regan and R. V. Smith, Satellite measurements of low energy electrons in the northern auroral zone, J. Geophys. Res. 69, 2721, 1964.

61. Gringauz, K. I., V. G. Kurt, V. I. Moroz, and I. C. Sklovskiy, 'Iskusstvennye Sputniki Zemli' Izd. AN SSSR, 6, 108, 1961; Planet. Space Sci. 9, 21, 1962.

62. O'Brien, B. J., J. A. Van Allen, C. D. Laughlin, and L. A. Frank, Absolute electron intensities in the heart of the earth's outer radiation zone, J. Geophys. Res. 67, 397-403, 1962.

63. O'Brien, B. J., and H. Taylor, High latitude geophysical studies with satellite Injun 3, 5. Auroras and their excitation, J. Geophys. Res. 69, 45-64, 1964.

64. Freeman, J. W., Detection of an intense flux of low energy protons or ions trapped in the inner radiation zone, J. Geophys. Res. 67, 921, 1962.

65. Hilton, H. H., J. R. Stevens, and A. L. Vampola, Observations of large fluxes of low energy electrons, Trans. Am. Geophys. Union 45, 602, 1964.

66. Frank, L. A., Observations of Magnetospheric Boundary Phenomena, University of Iowa Report 65-32, August 1965.

Table 1

Location	Particle Flux	Time to Damage
Solar Wind	J_p(~1Kev) $\sim 10^8 \frac{\text{protons}}{\text{cm}^2\text{-sec}}$	$\sim 10^8$ sec = 3 years
Transition Zone	J_p(~1Kev) $\sim 10^8 \frac{\text{protons}}{\text{cm}^2\text{-sec}}$	$\sim 10^8$ sec
	J_e(.1 to 50Kev) $\sim 10^9 \frac{\text{electrons}}{\text{cm}^2\text{-sec}}$	$\sim 10^6$ sec = 10 days
Outer Belt	J_p(>.1Mev) $\sim 10^8 \frac{\text{protons}}{\text{cm}^2\text{-sec}}$	$\sim 10^6$ sec = 10 days
	J_e(~.1Mev) $\sim 10^8 \frac{\text{electrons}}{\text{cm}^2\text{-sec}}$	$\sim 10^7$ sec = 3 months
Inner Belt	J_p*(~10Kev) $\sim 10^{10} \frac{\text{protons}}{\text{cm}^2\text{-sec}}$	$\sim 10^6$ sec = 10 days
Storm Time	J_p*(~10Kev) $\sim 10^{11} \frac{\text{protons}}{\text{cm}^2\text{-sec}}$	$\sim 10^5$ sec = 1 day
Aurora	J_e(~10Kev) $\sim 10^{11} \frac{\text{electrons}}{\text{cm}^2\text{-sec}}$	$\sim 10^4$ sec = 3 hours

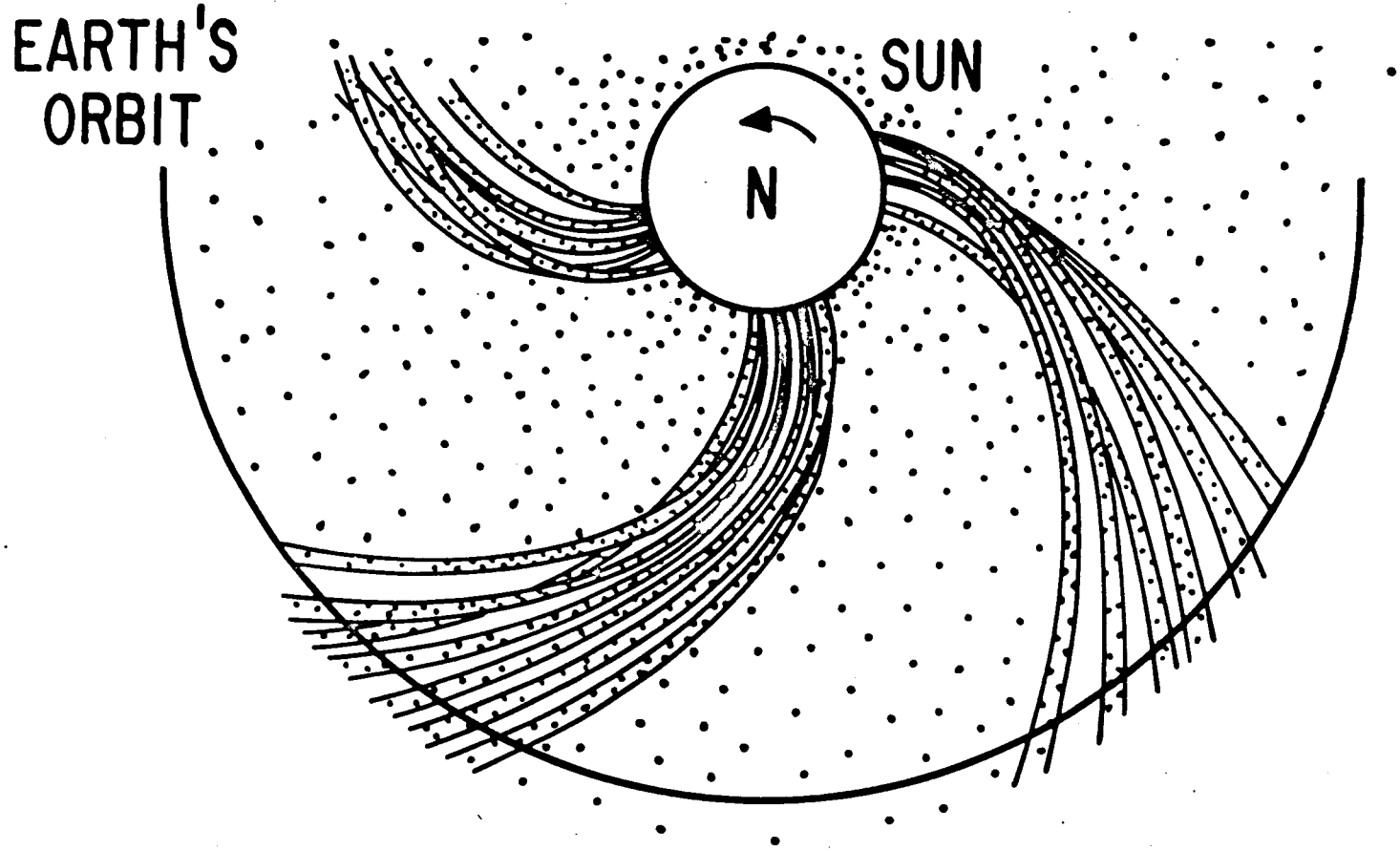

Figure 1

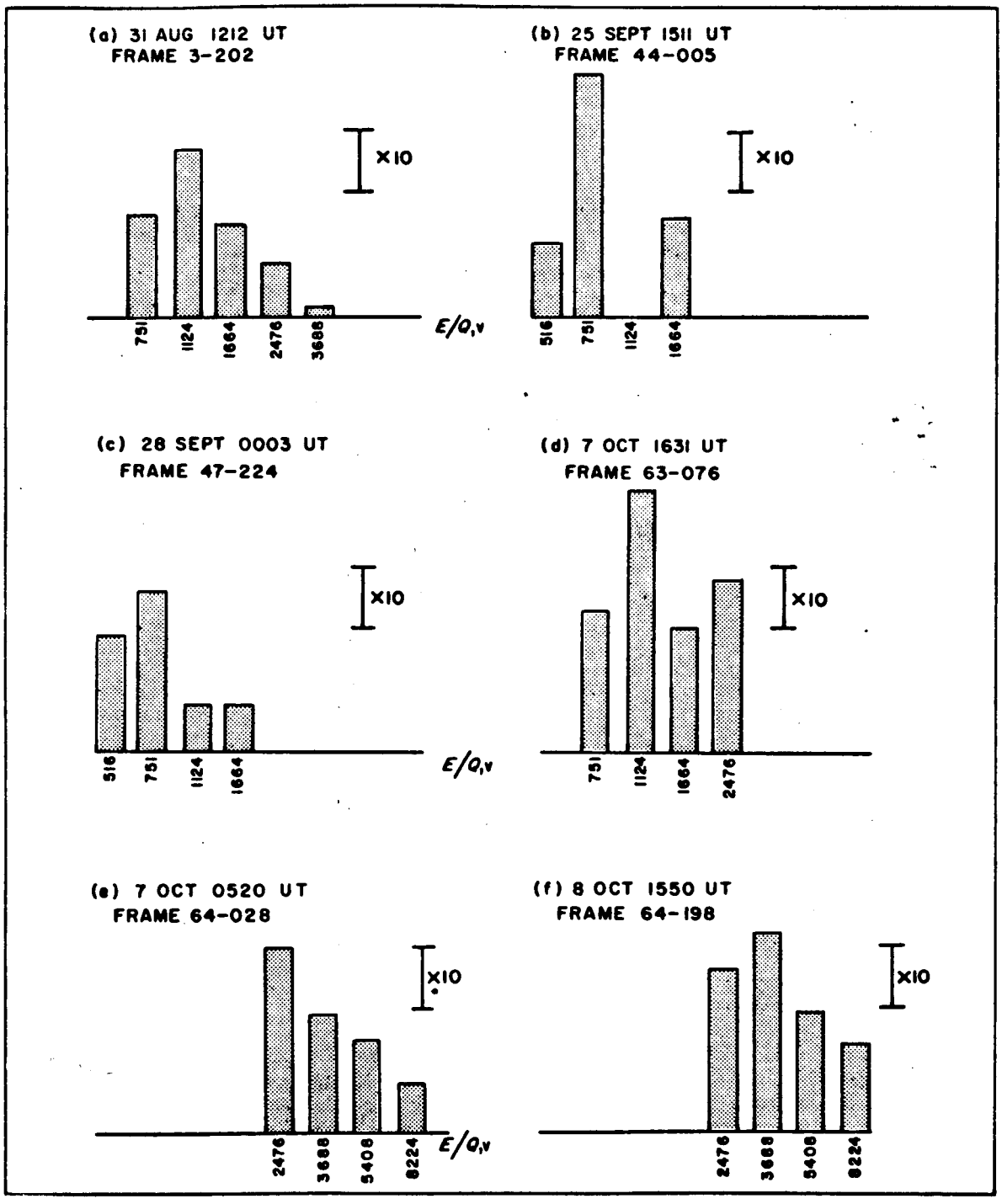
(a) 31 AUG 1212 UT
FRAME 3-202
X10
751
1124
1664
2476
3688
E/Q,V
(b) 25 SEPT 1511 UT
FRAME 44-005
X10
516
751
1124
1664
(c) 28 SEPT 0003 UT
FRAME 47-224
X10
516
751
1124
1664
E/Q,V
(d) 7 OCT 1631 UT
FRAME 63-076
X10
751
1124
1664
2476
(e) 7 OCT 0520 UT
FRAME 64-028
X10
2476
3688
5408
8224
E/Q,V
(f) 8 OCT 1550 UT
FRAME 64-198
X10
2476
3688
5408
8224

Figure 2

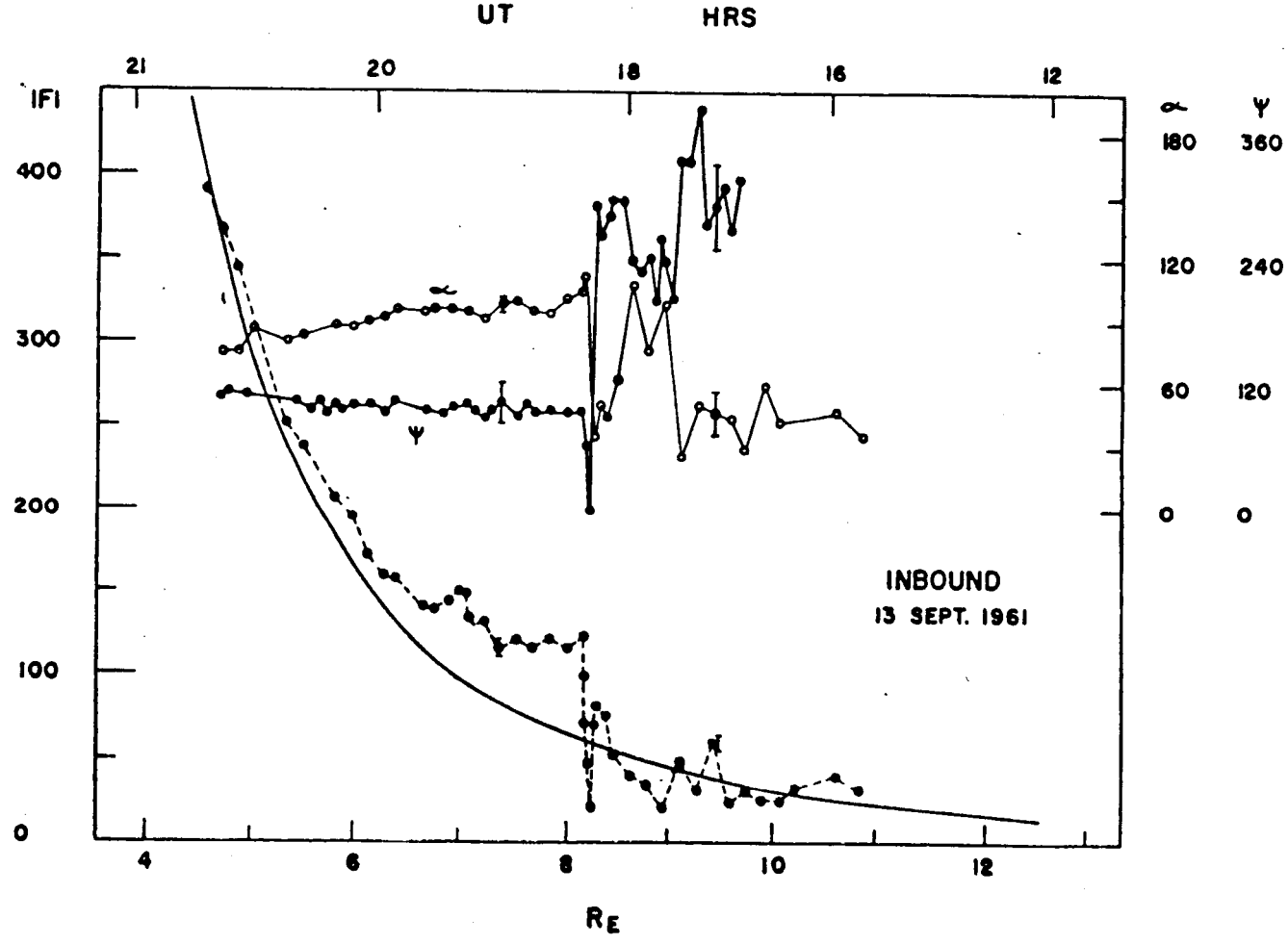
UT HRS
21
20
18
16
12
|F|
400
300
200
100
0
α
ψ
180
360
120
240
60
120
0
0
INBOUND
13 SEPT. 1961
4
6
8
10
12
R_E

Figure 3

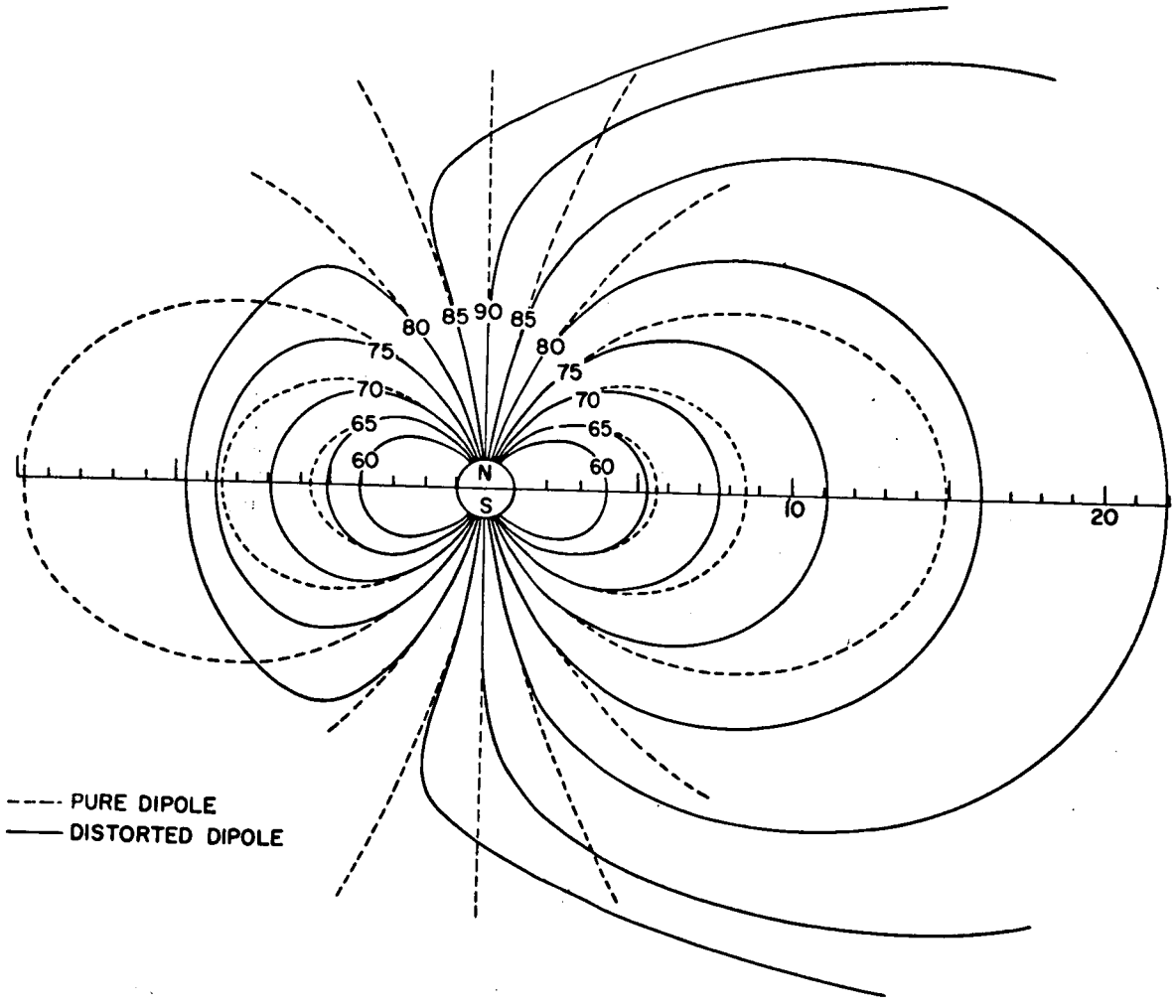
90
85
85
80
80
75
75
70
70
65
65
60
60
N
S
10
20
PURE DIPOLE
DISTORTED DIPOLE

Figure 4

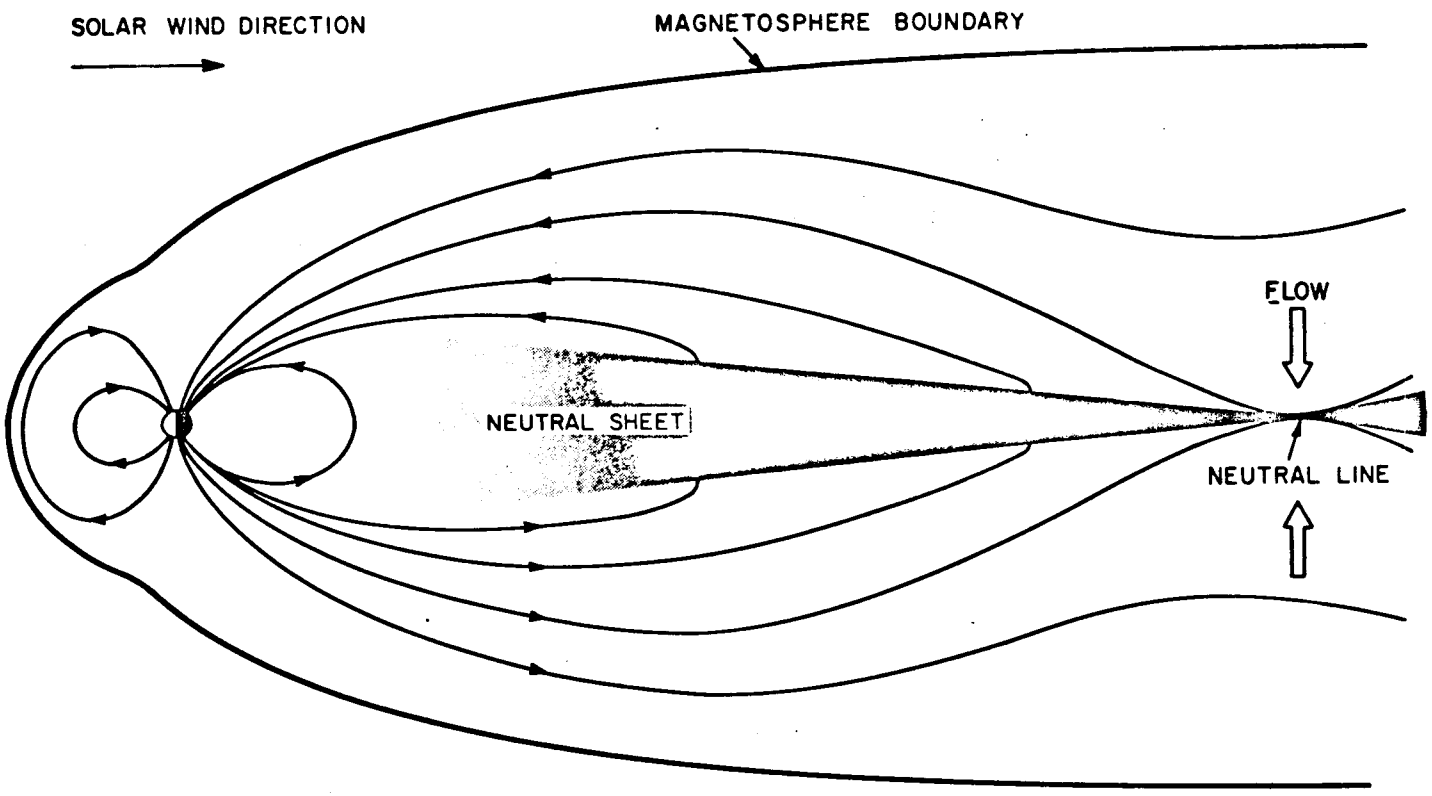
SOLAR WIND DIRECTION
MAGNETOSPHERE BOUNDARY
FLOW
NEUTRAL SHEET
NEUTRAL LINE

Figure 5

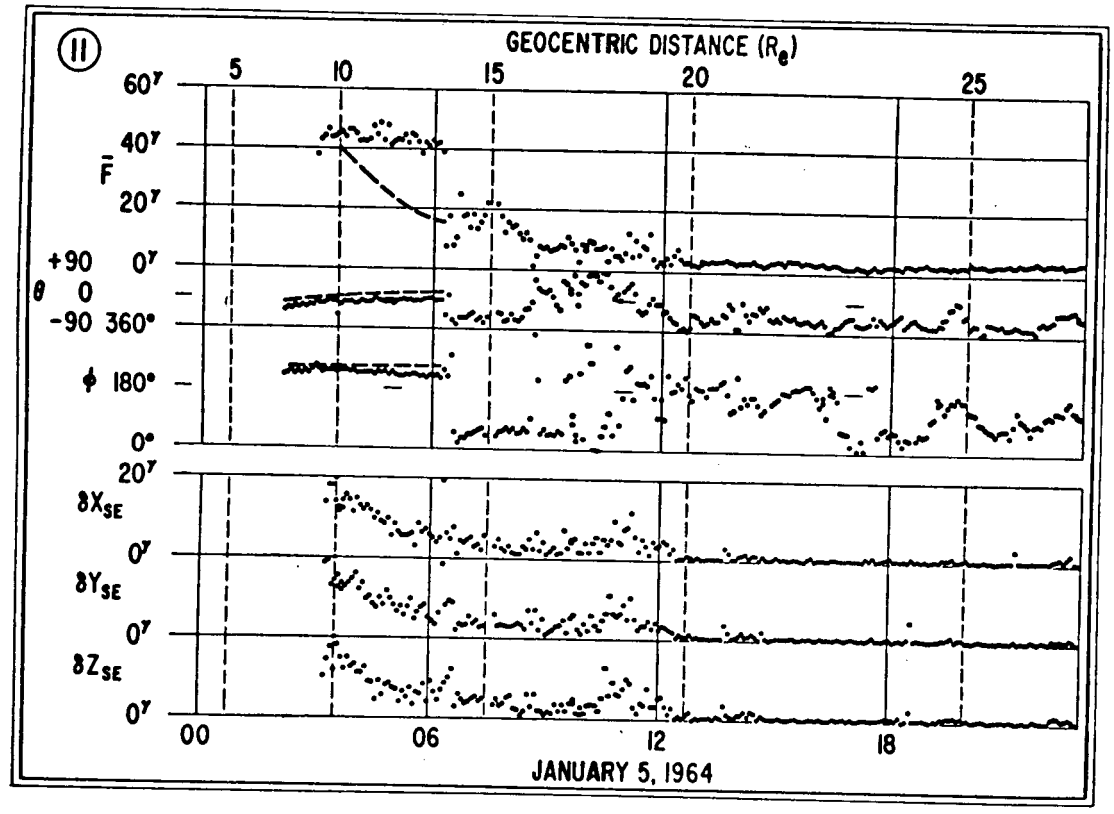
(11)
GEOCENTRIC DISTANCE (R_e)
5
10
15
20
25
60γ
40γ
$\bar{F}$
20γ
+90
0γ
θ 0
-90
360°
φ 180°
0°
20γ
δX_{SE}
0γ
δY_{SE}
0γ
δZ_{SE}
0γ
00
06
12
18
JANUARY 5, 1964

Figure 6

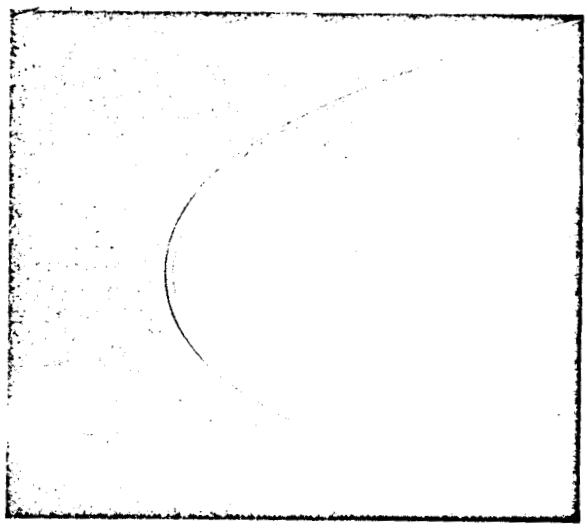

—A sphere in a supersonic wind tunnel showing a detached shock wave upstream from the object.

FIGURE 7

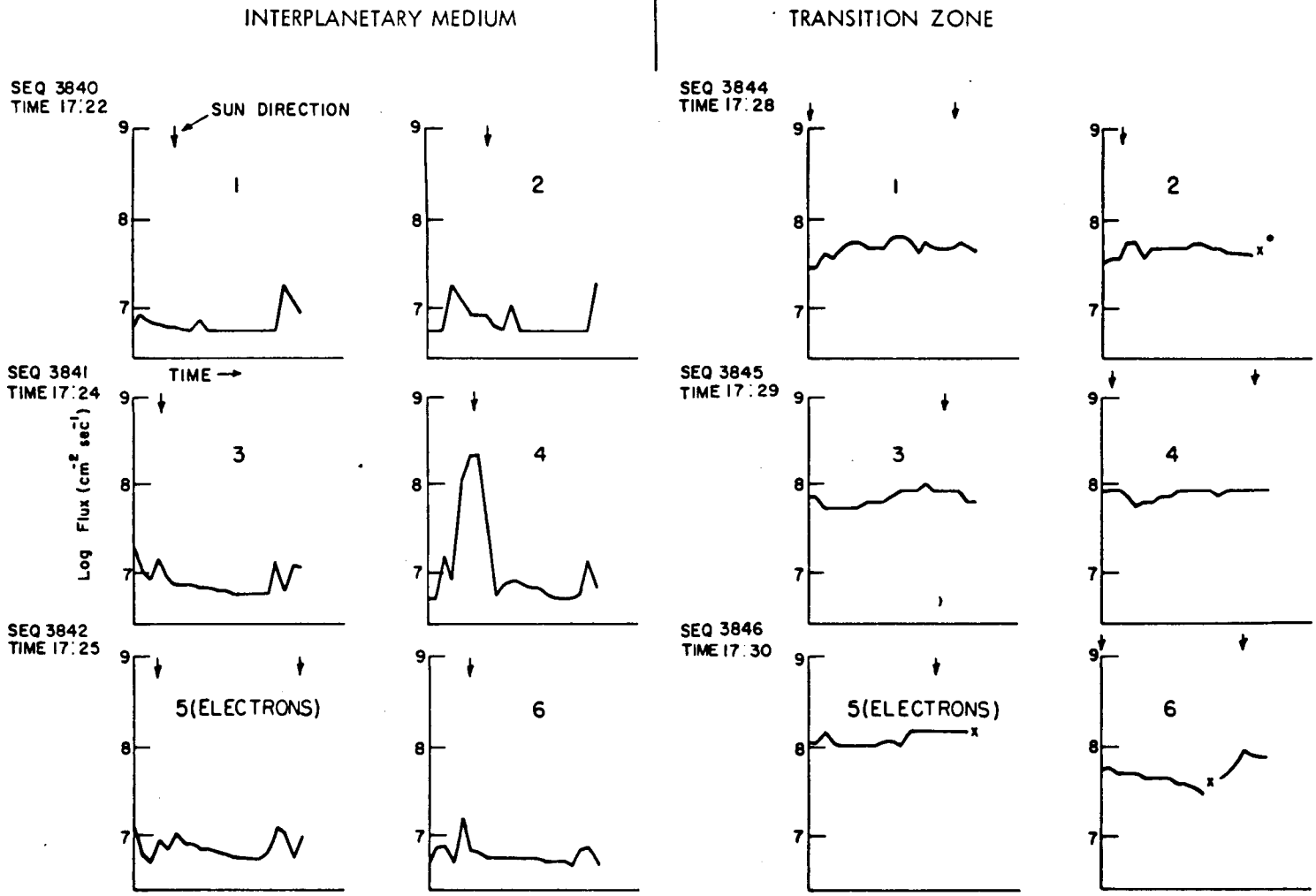
INTERPLANETARY MEDIUM
TRANSITION ZONE
SEQ 3840
TIME 17:22
SUN DIRECTION
SEQ 3841
TIME 17:24
TIME →
Log Flux (cm⁻² sec⁻¹)
SEQ 3842
TIME 17:25
5(ELECTRONS)
SEQ 3844
TIME 17:28
SEQ 3845
TIME 17:29
SEQ 3846
TIME 17:30
5(ELECTRONS)
1
2
3
4
6
9
8
7

Figure 8

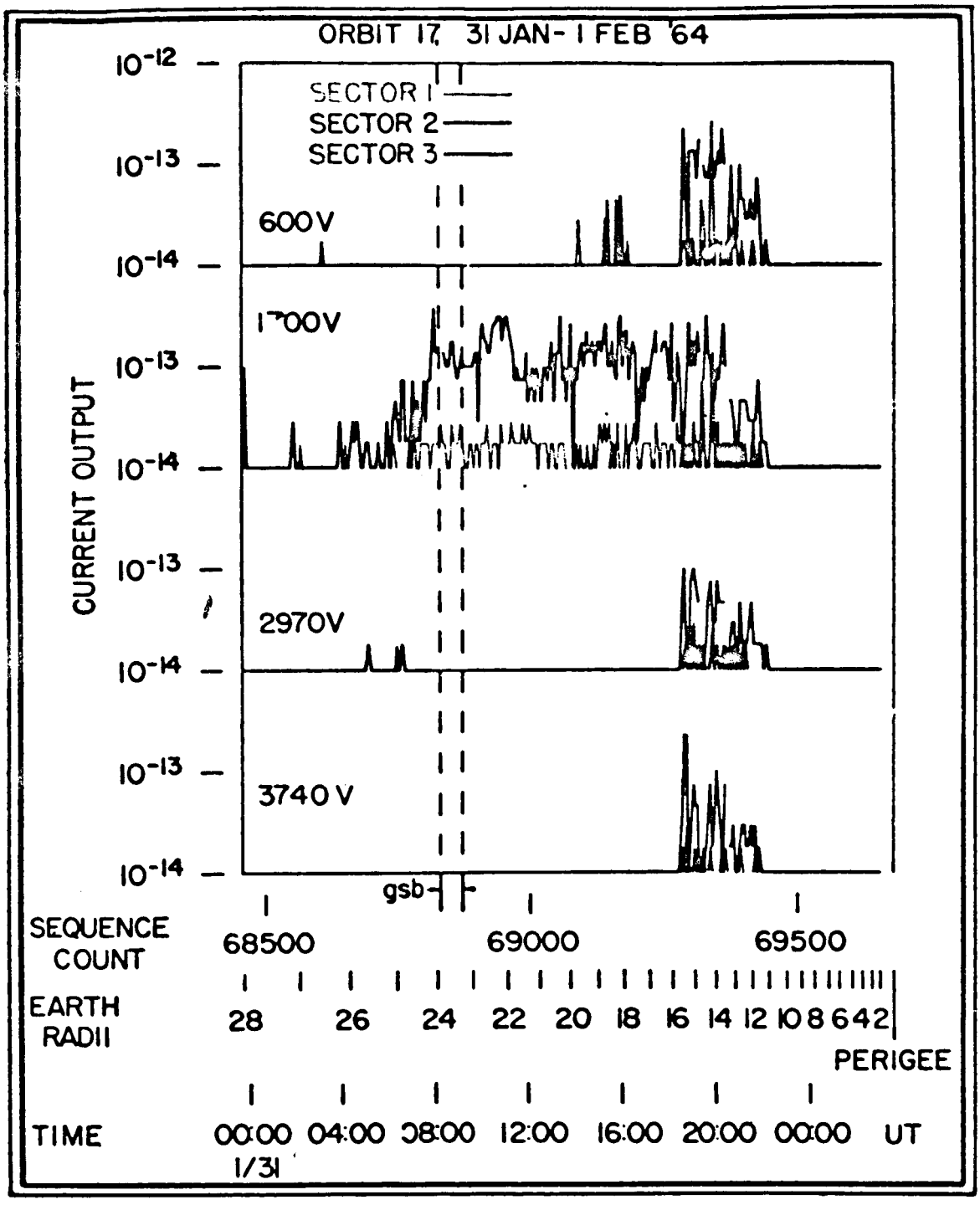
ORBIT 17, 31 JAN - 1 FEB '64
SECTOR 1
SECTOR 2
SECTOR 3
600V
1700V
2970V
3740V
CURRENT OUTPUT
10-12
10-13
10-14
gsb
SEQUENCE COUNT
68500
69000
69500
EARTH RADII
28 26 24 22 20 18 16 14 12 10 8 6 4 2
PERIGEE
TIME
00:00 04:00 08:00 12:00 16:00 20:00 00:00 UT
1/31

Figure 9

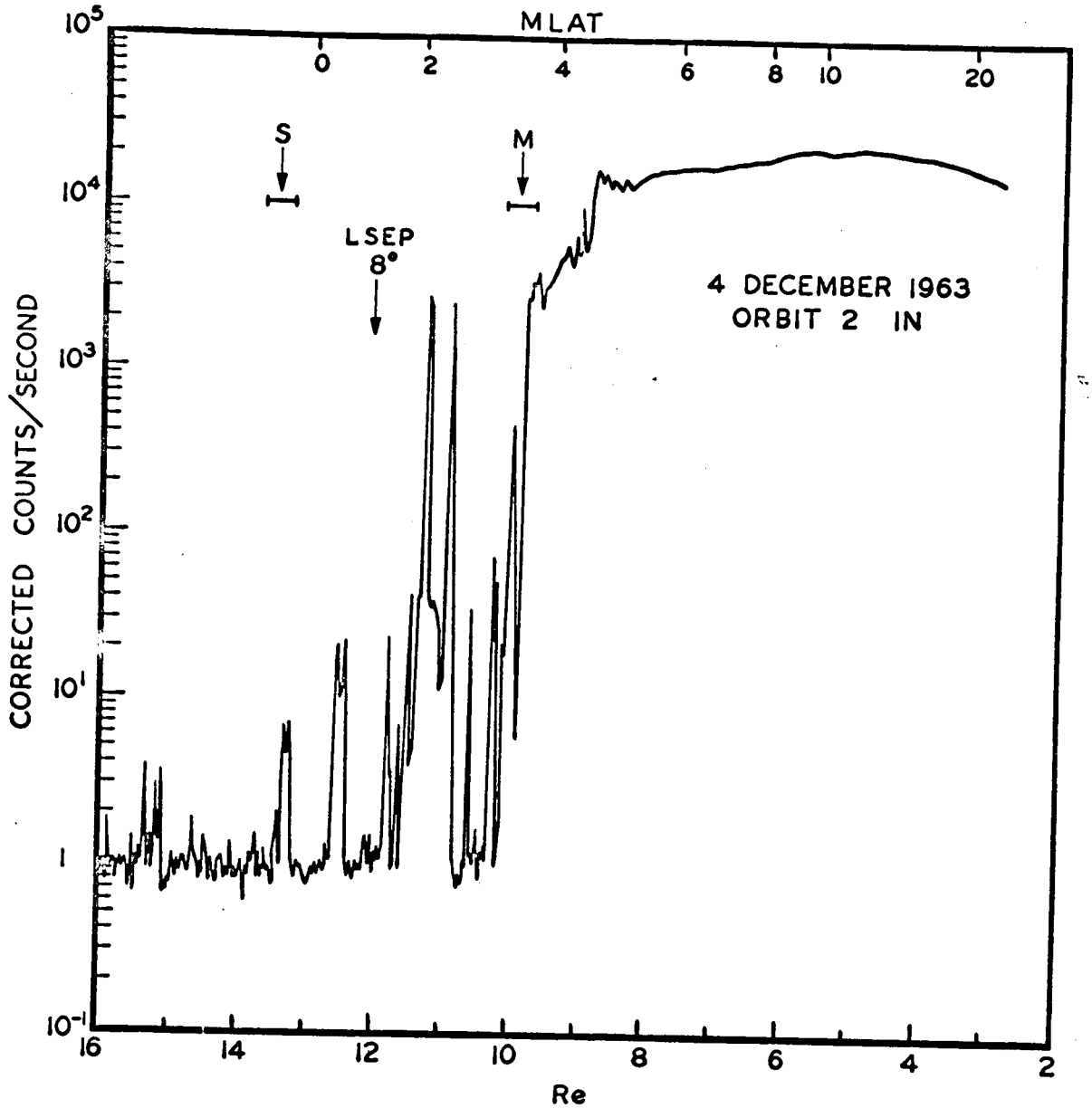
MLAT
0
2
4
6
8
10
20
S
M
LSEP
8°
4 DECEMBER 1963
ORBIT 2 IN
CORRECTED COUNTS/SECOND
10^5
10^4
10^3
10^2
10^1
1
10^{-1}
16
14
12
10
8
6
4
2
Re

Figure 10

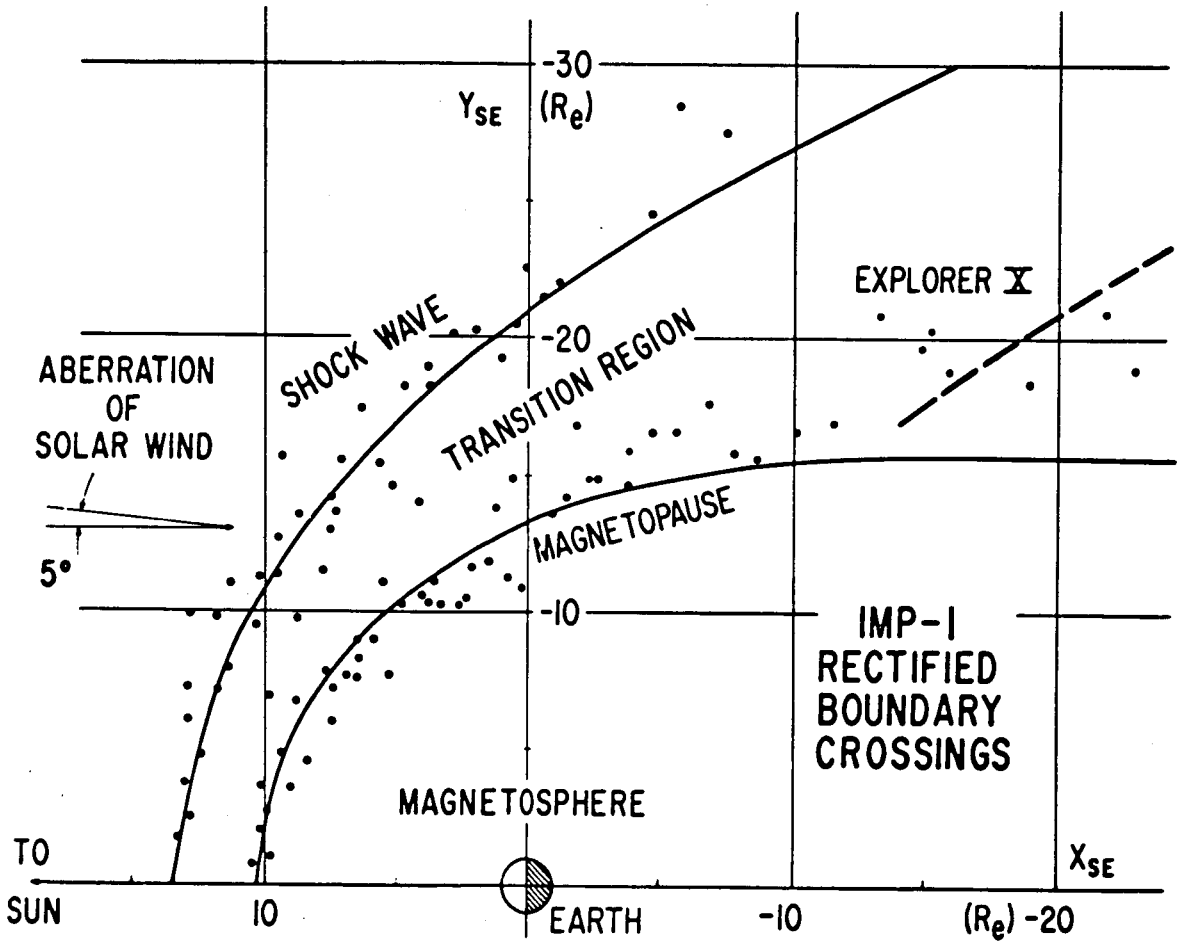
-30
Y_{SE} (R_e)
-20
-10
EXPLORER X
SHOCK WAVE
TRANSITION REGION
ABERRATION
OF
SOLAR WIND
5°
MAGNETOPAUSE
IMP-I
RECTIFIED
BOUNDARY
CROSSINGS
MAGNETOSPHERE
TO
SUN
10
EARTH
-10
(R_e) -20
X_{SE}

Figure 11

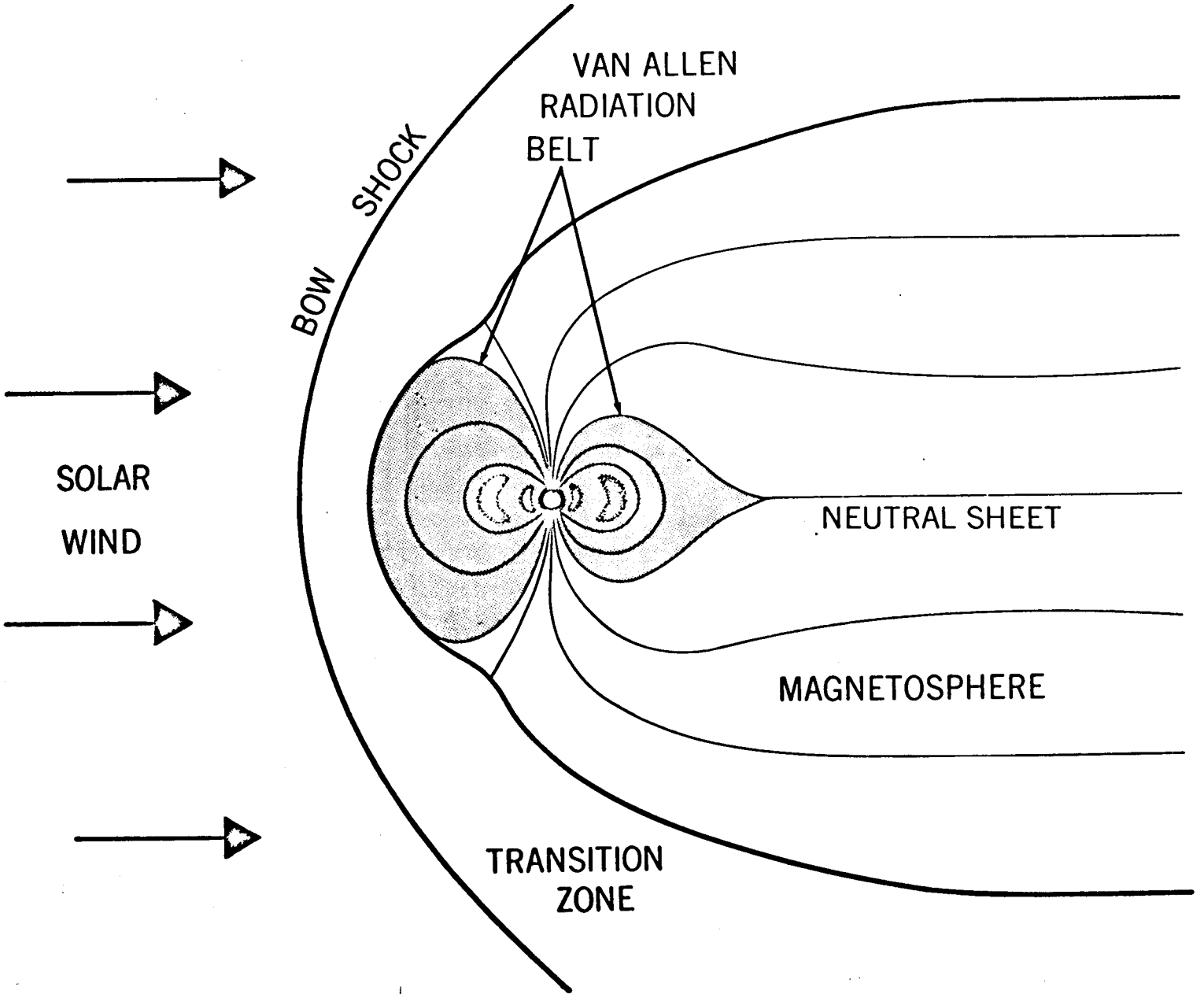
VAN ALLEN
RADIATION
BELT
BOW SHOCK
SOLAR
WIND
NEUTRAL SHEET
MAGNETOSPHERE
TRANSITION
ZONE

Figure 12

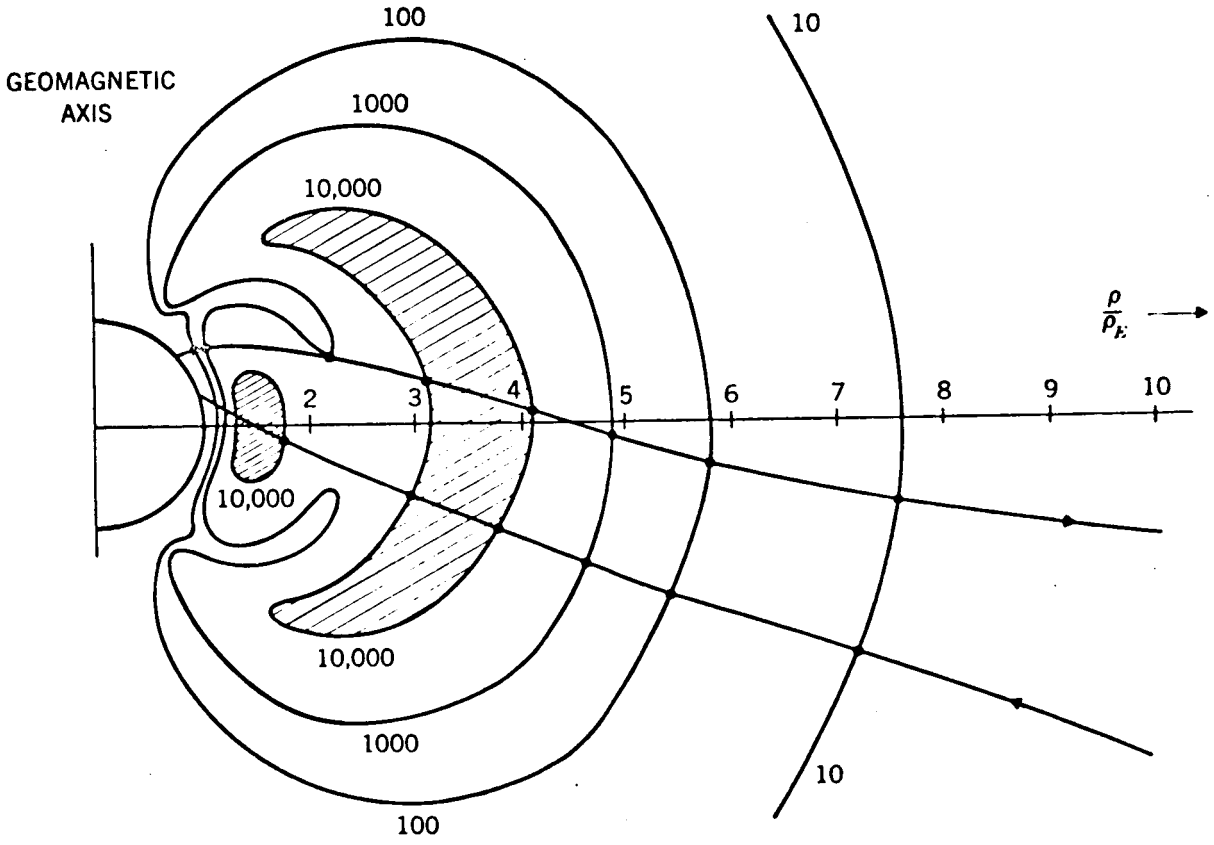
GEOMAGNETIC
AXIS
100
1000
10,000
10
$\frac{\rho}{\rho_E}$
2
3
4
5
6
7
8
9
10
10,000
10,000
1000
100
10

Figure 13

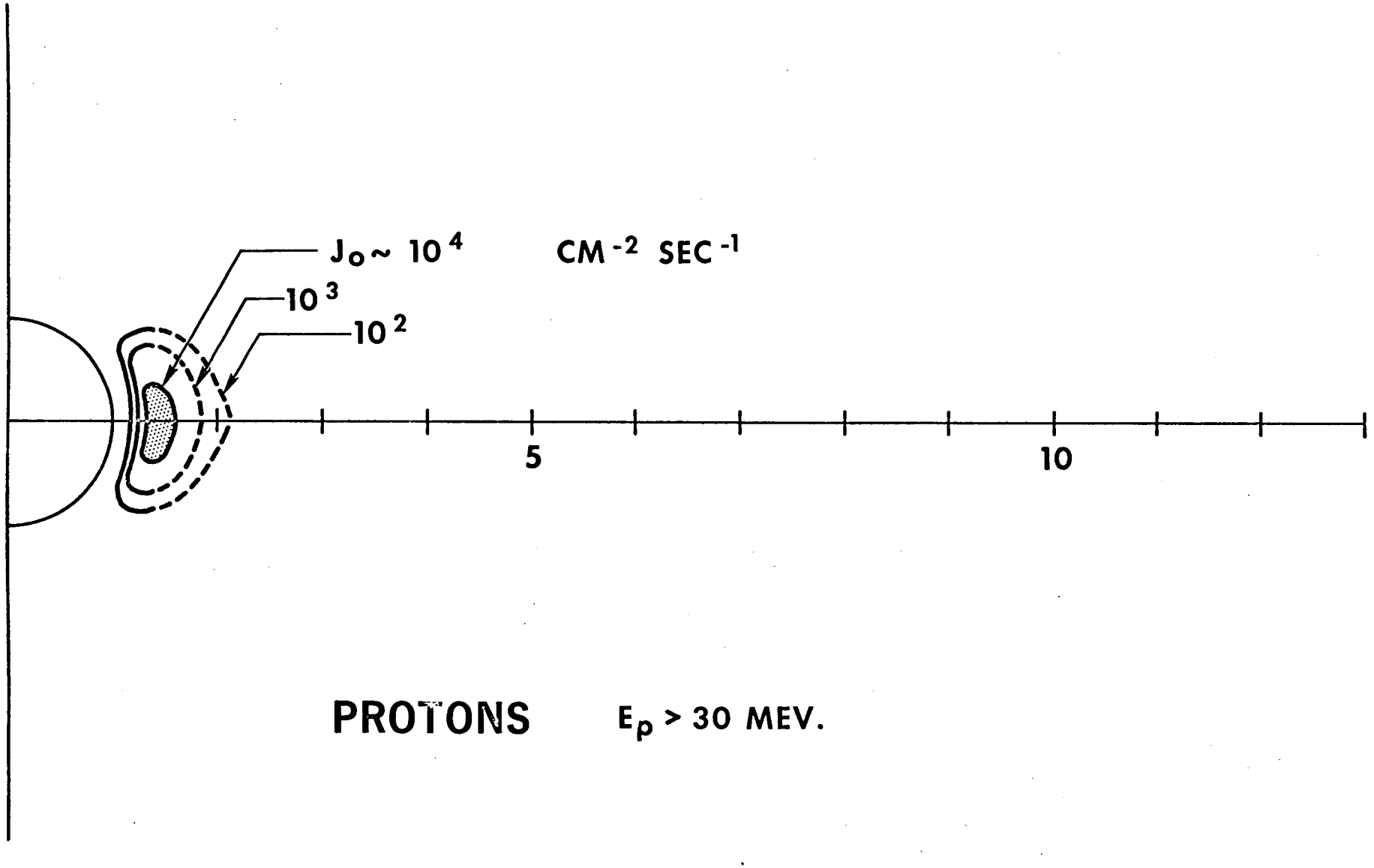

Figure 14

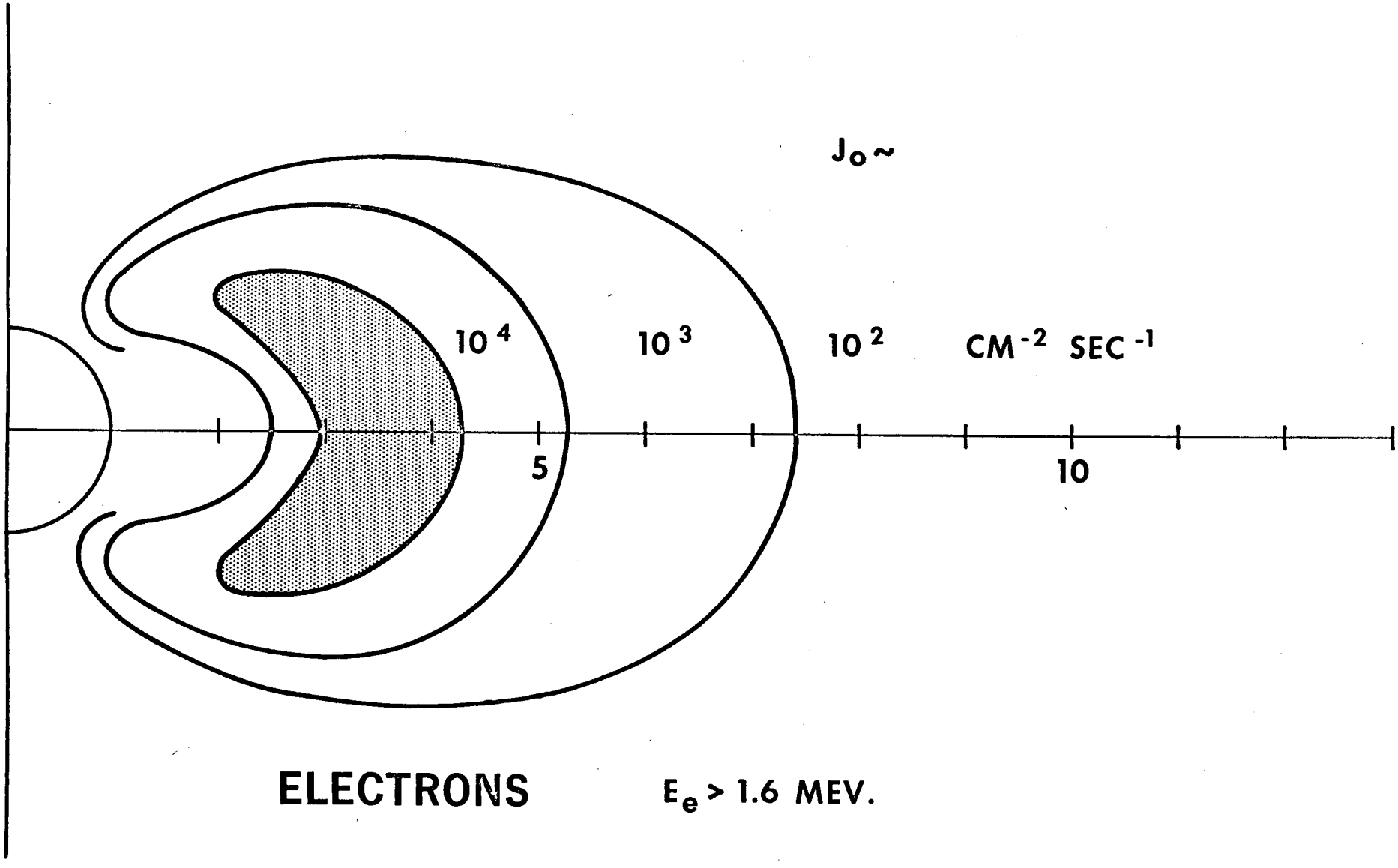

Figure 15

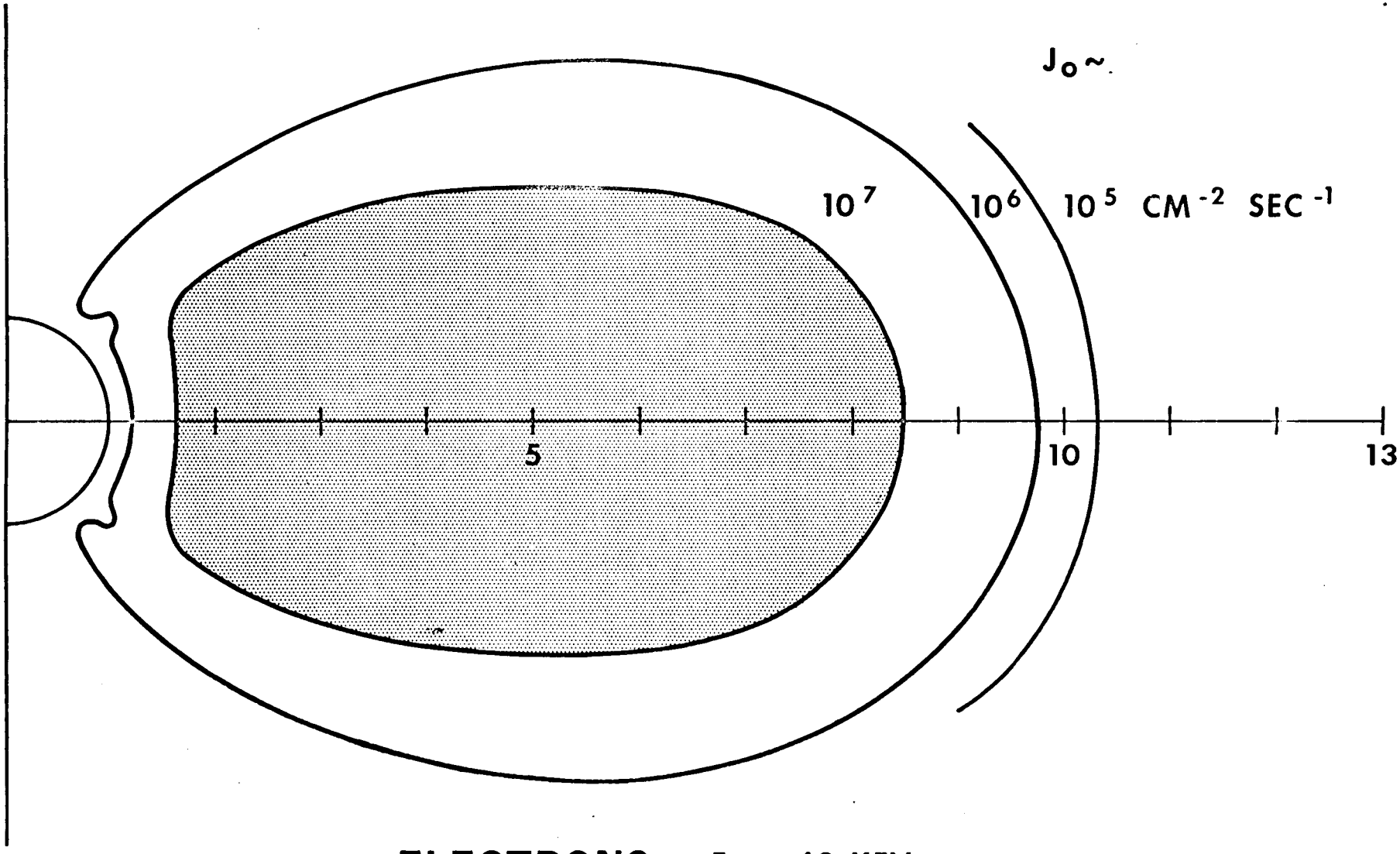

Figure 16

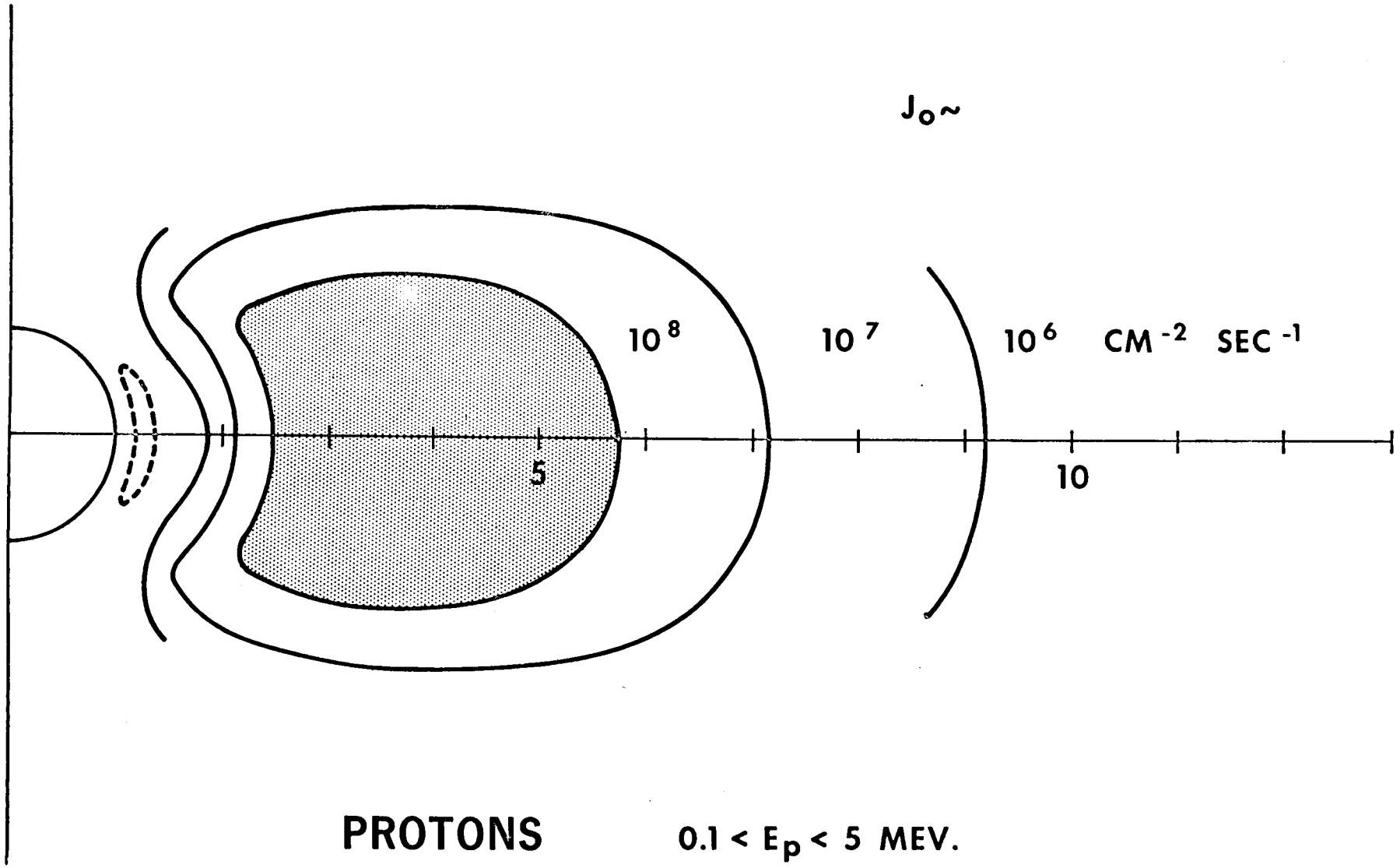

Figure 17

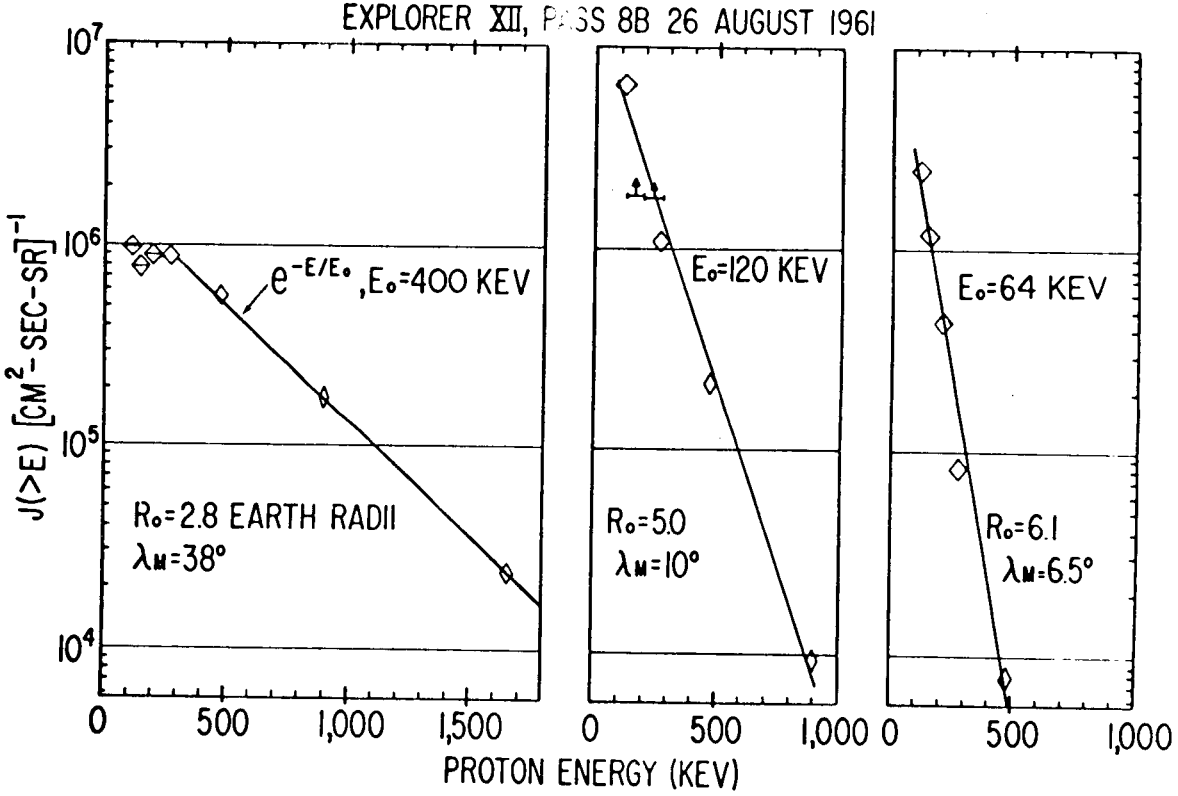
EXPLORER XII, PASS 8B 26 AUGUST 1961
J(>E) [CM²-SEC-SR]⁻¹
10⁷
10⁶
10⁵
10⁴
e^-E/E₀, E₀=400 KEV
R₀=2.8 EARTH RADII
λM=38°
E₀=120 KEV
R₀=5.0
λM=10°
E₀=64 KEV
R₀=6.1
λM=6.5°
0
500
1,000
1,500
PROTON ENERGY (KEV)

Figure 18

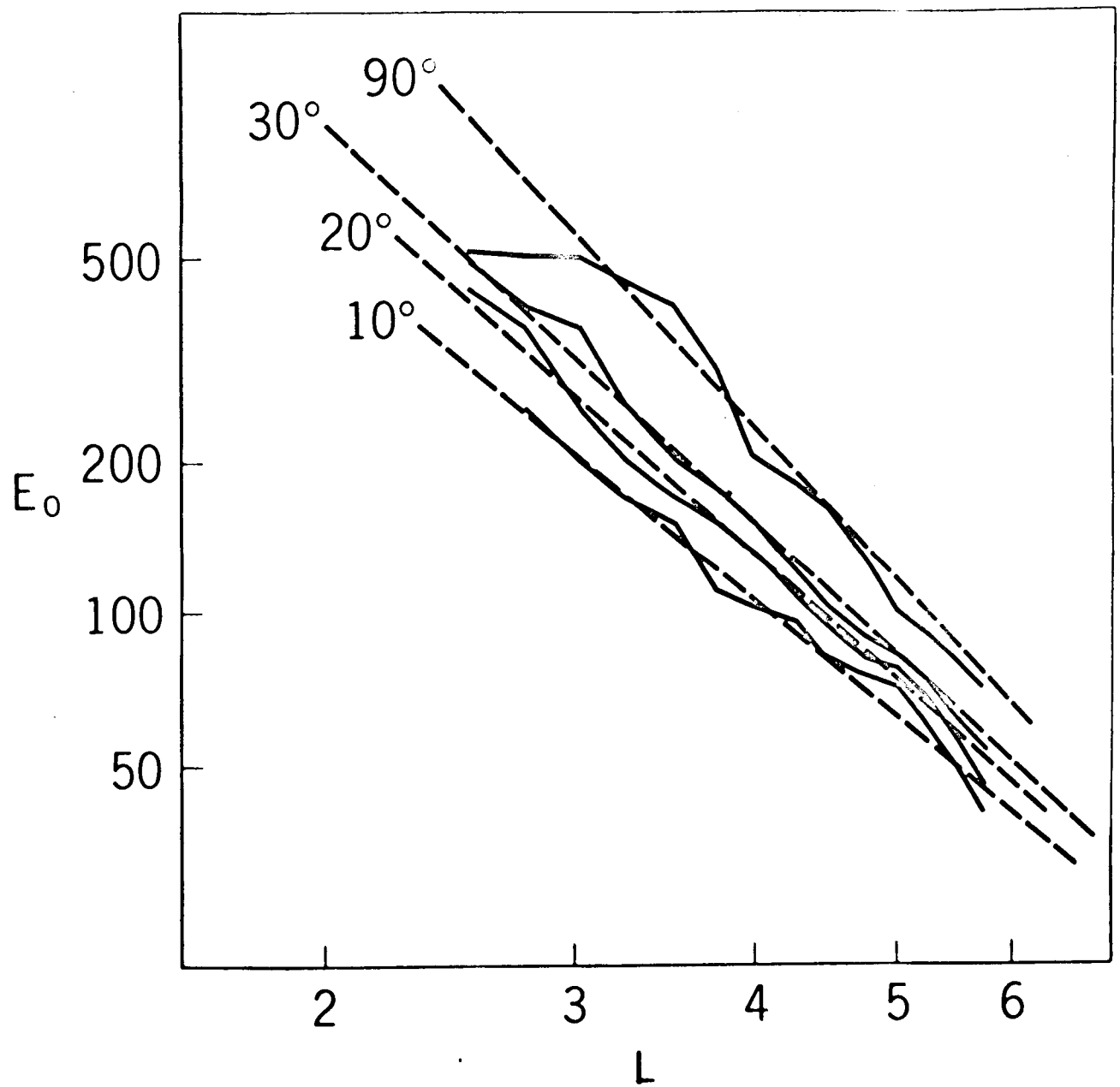

Figure 19

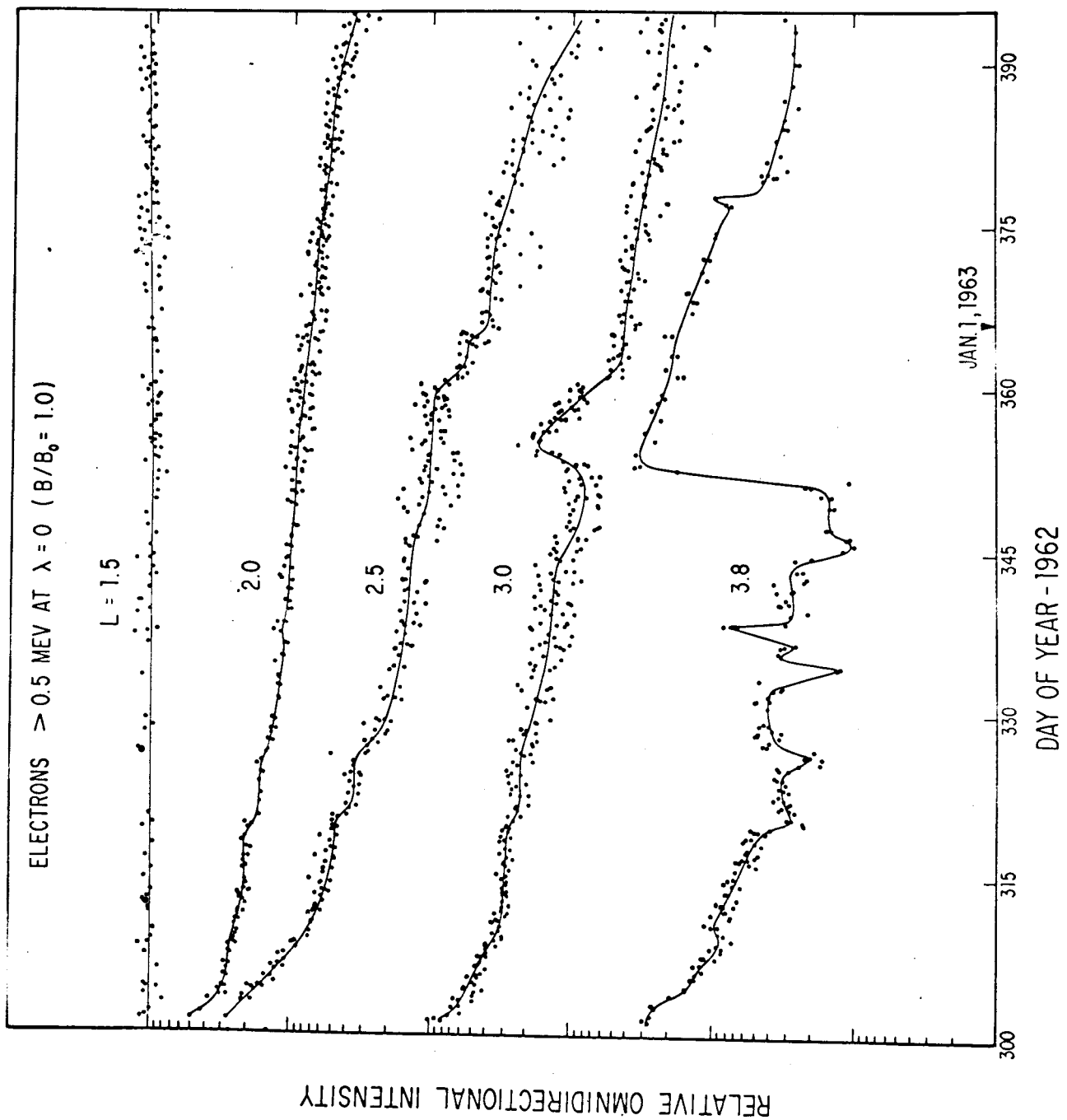
ELECTRONS > 0.5 MEV AT λ = 0 (B/B₀ = 1.0)
L = 1.5
2.0
2.5
3.0
3.8
JAN. 1, 1963
300
315
330
345
360
375
390
DAY OF YEAR - 1962
RELATIVE OMNIDIRECTIONAL INTENSITY

Fig. 20

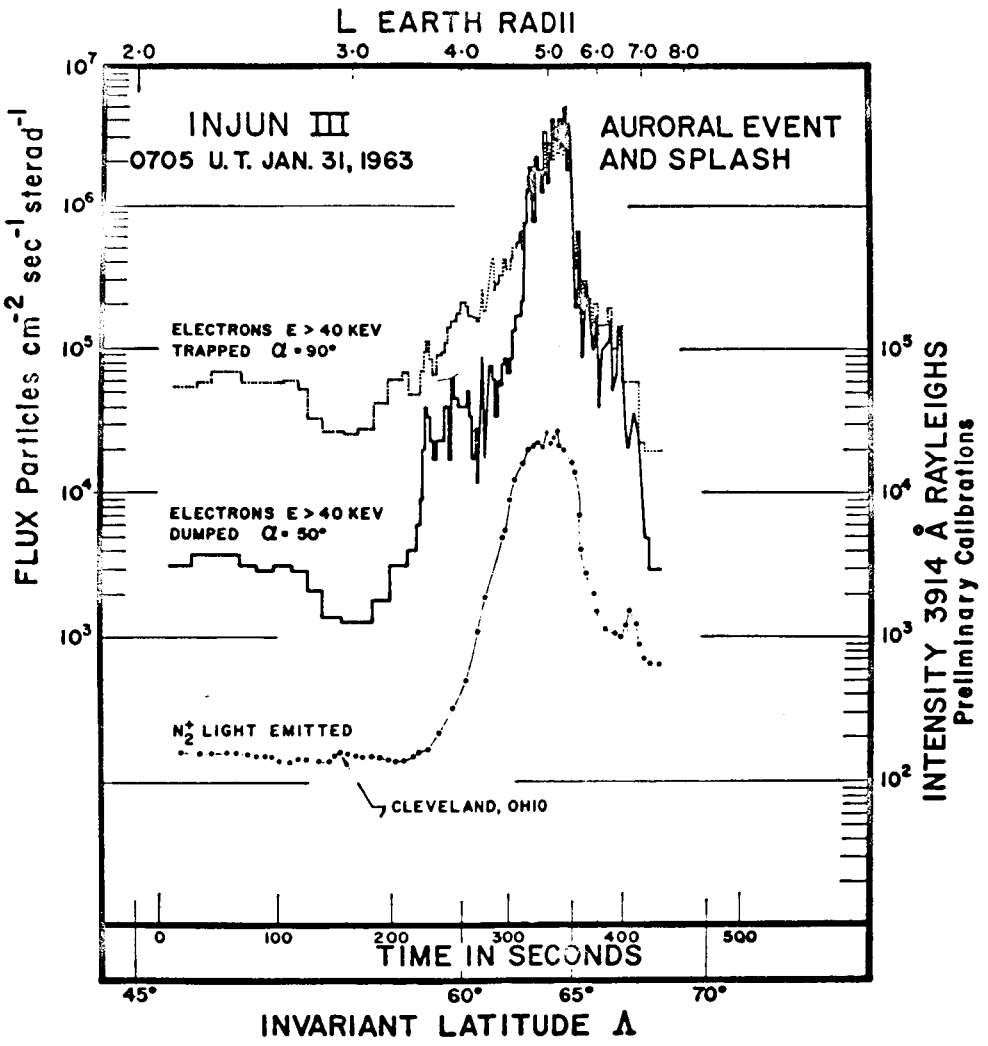
L EARTH RADII
2·0
3·0
4·0
5·0
6·0
7·0
8·0
INJUN III
0705 U.T. JAN. 31, 1963
AURORAL EVENT
AND SPLASH
ELECTRONS E > 40 KEV
TRAPPED α = 90°
ELECTRONS E > 40 KEV
DUMPED α = 50°
N2+ LIGHT EMITTED
CLEVELAND, OHIO
FLUX Particles cm-2 sec-1 sterad-1
INTENSITY 3914 Å RAYLEIGHS
Preliminary Calibrations
TIME IN SECONDS
INVARIANT LATITUDE Λ

Figure 21

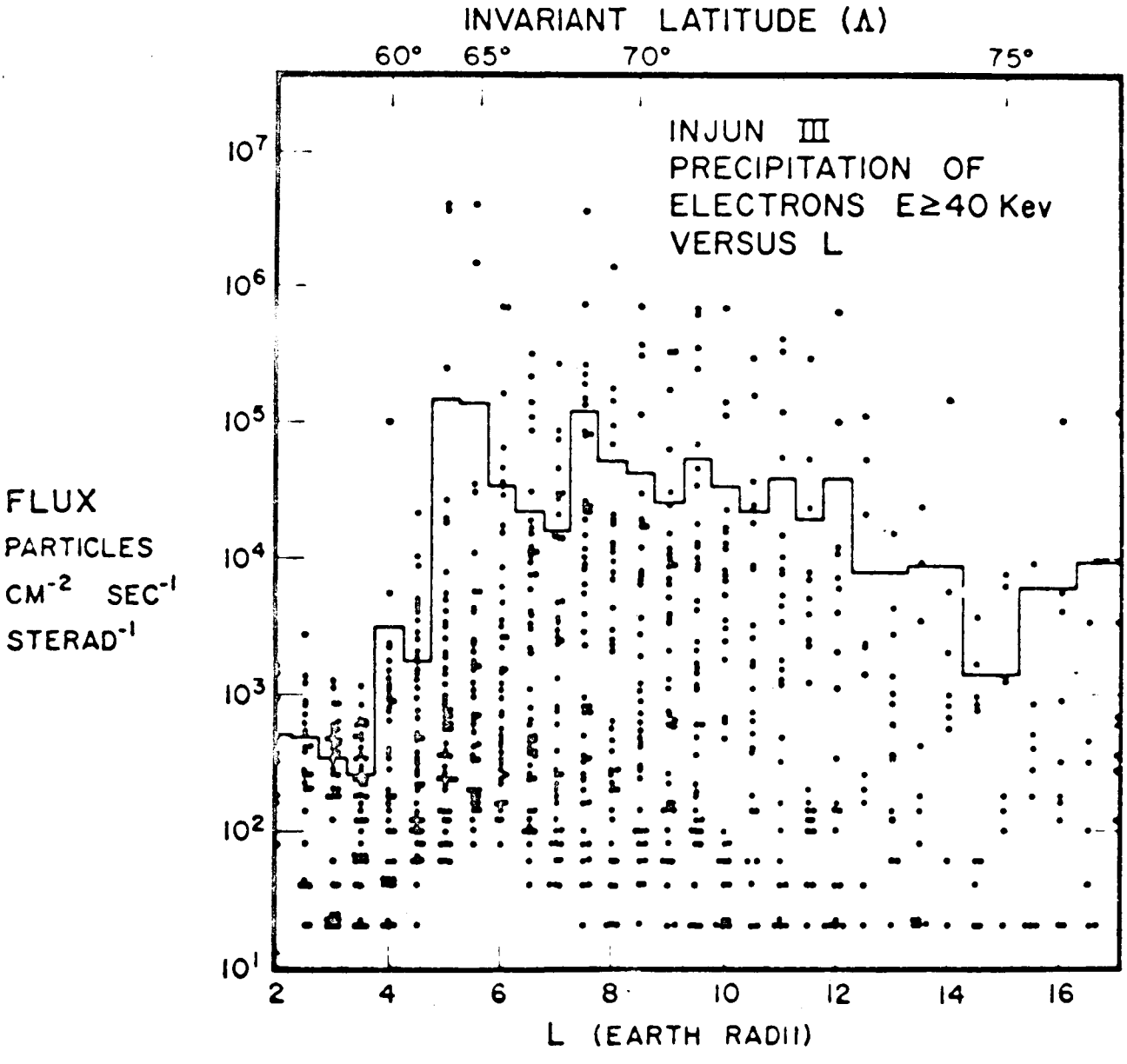
INVARIANT LATITUDE (Λ)
60°
65°
70°
75°
INJUN III
PRECIPITATION OF
ELECTRONS E≥40 Kev
VERSUS L
FLUX
PARTICLES
CM-2 SEC-1
STERAD-1
10^7
10^6
10^5
10^4
10^3
10^2
10^1
2
4
6
8
10
12
14
16
L (EARTH RADII)

Figure 22

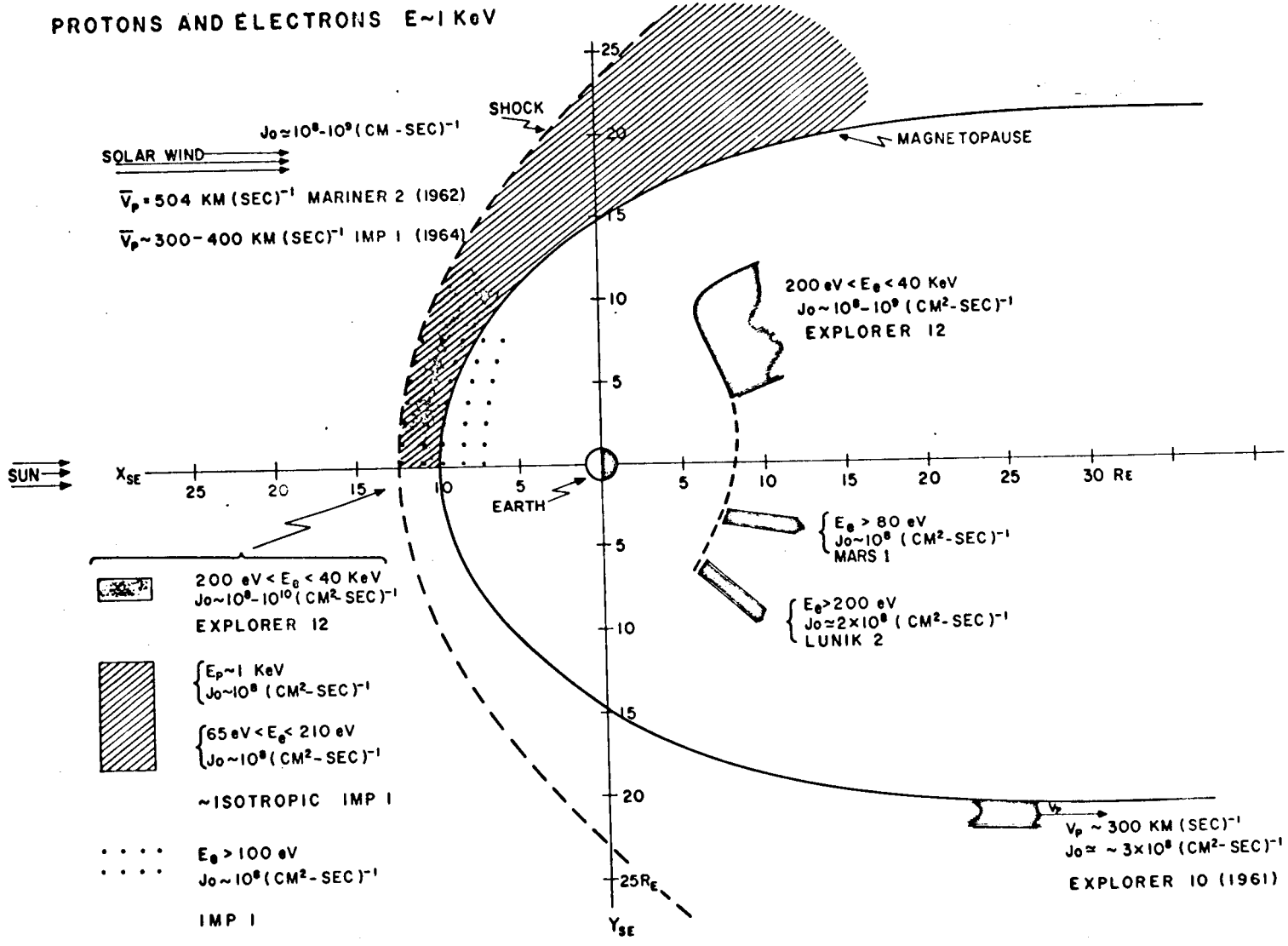
PROTONS AND ELECTRONS E~1 KeV
SHOCK
MAGNETOPAUSE
Jo≃10⁸-10⁹ (CM-SEC)⁻¹
SOLAR WIND
V̄p = 504 KM (SEC)⁻¹ MARINER 2 (1962)
V̄p ~ 300-400 KM (SEC)⁻¹ IMP 1 (1964)
200 eV < Ee < 40 KeV
Jo ~ 10⁸-10⁹ (CM²-SEC)⁻¹
EXPLORER 12
SUN
XSE
EARTH
Ee > 80 eV
Jo~10⁸ (CM²-SEC)⁻¹
MARS 1
Ee>200 eV
Jo≃2×10⁸ (CM²-SEC)⁻¹
LUNIK 2
200 eV < Ee < 40 KeV
Jo~10⁸-10¹⁰ (CM²-SEC)⁻¹
EXPLORER 12
Ep~1 KeV
Jo~10⁸ (CM²-SEC)⁻¹
65 eV < Ee < 210 eV
Jo~10⁸ (CM²-SEC)⁻¹
~ISOTROPIC IMP 1
Ee > 100 eV
Jo~10⁸ (CM²-SEC)⁻¹
IMP 1
Vp ~ 300 KM (SEC)⁻¹
Jo≃ ~3×10⁸ (CM²-SEC)⁻¹
EXPLORER 10 (1961)
25RE
YSE
30 RE

Figure 23